Master Thesis in Geosciences

Recent Chemical Changes in Gardermoen Aquifer

Effect of Cation Exchange Processes on the composition of groundwater

Temesgen G. Kahsay

UNIVERSITY OF OSLO

FACULTY OF MATHEMATICS AND NATURAL SCIENCES

Everything comes from him;
Everything happens through him;
Everything ends up in him.
Always glory! Always praise!
Yes. Yes. Yes.

The Message Bible

Recent Chemical Changes in Gardermoen Aquifer

Effect of Cation Exchange Processes on the composition of groundwater

Temesgen G. Kahsay

Master Thesis in Geosciences

Discipline: Environmental Geology and Geohazards

Department of Geosciences

Faculty of Mathematics and Natural Sciences

UNIVERSITY OF OSLO

June 2006

Abstract

Recent analysis of water samples from Gardermoen Aquifer, the largest unconfined groundwater reservoir in Norway, revealed increasing trend of calcium and magnesium concentrations. The international Oslo Airport, situated above the aquifer, discharges several volume of runoff contaminated by deicing chemicals into the subsurface. Propylene glycol and Sodium formate are the principal components of deicing chemicals widely used in the airport during winter season. Sodium formate is a soluble compound and readily dissociates in to its ions upon reaching the groundwater.

Soil samples were taken from borehole near the eastern runway in the airport ground. These samples were analysed with respect to mineralogical composition, grain size distribution, carbon content, exchangeable ions and cation exchange capacity. Data from chemical analysis of snow collections and previous water samples are used to identify the major processes that govern the increasing trend of calcium and magnesium.

Cation exchange capacity of the soils was determined by saturating the sample with a NH4NO3 and SrCl2 solutions independently. The results obtained range between 1.5-3.5 meq/l, with calcium being the dominant ion on the exchange sites. Geochemical modelling also strengthens the evidence of cation exchange processes being the dominant factors involved in the recent changes in groundwater chemistry.

Key words: Cation exchange capacity, deicing chemicals, geochemical modelling

Acknowledgment

The successful completion of this Masters thesis is due to the effort of many people. First I would like to thank my advisor Per Aagaard (Prof) for his continual guidance and constructive follow-up during the course of this thesis. Thank you Per for making yourself available any time I want.

My thanks also go to Bente Wejden from Oslo International Airport (OSL), who provide me the data I used and facilitate my activities in the airport.

I greatly appreciate the efforts of Mufak Naoroz, Berit Løken Berg and Turid Winje all from the Department of Geosciences, who carefully carried out laboratory works and helped me to get the results on time. I also thank Marit Carlsen (Student Advisor) and all the staff in the department who frequently kept me up-to-date and smoothly sorted out a lot of paper works involved in my two year stay in the department.

I also would like to extend my gratitude to Anja Sundal, Beniam (Ben) and all friends who socially make my stay in Norway comfortable.

Finally I owe much to all Norwegian tax payers, who made it possible for me to get the scholarship and continue my studies and learn in Norway. Takk Norge!

Table of contents **Page**

List of Annexes

List of figures and tables **Page**

List of Tables

1. Introduction

In many parts of the world groundwater is one of the most important sources of water supply. With ever-increasing population of the world the quantity and quality of this vulnerable resource has been falling and deteriorating. The discovery of widespread groundwater contamination in the last few decades and growing awareness of the importance of this resource has led to extensive efforts throughout the world to protect clean groundwater and remediate contaminated aquifers (31).

The field of groundwater has received tremendous attention because understanding the systems involved in the evolution of groundwater greatly assists its proper utilisation and preservation. Aquifer protection requires effective groundwater monitoring and remediation requires adequate site characterization to identify the sources, levels and mobility of contaminating substances.

Groundwater acquires its chemical characteristic by dissolution and by chemical reactions with solids, liquids and gases with which it has come in contact during the various parts of the hydrological cycle (25). Several endeavours undertaken by human beings have introduced disruptive processes that alter the overall groundwater system.

In Norway only less than 15% of the population uses groundwater as a source for drinking water (12). Even if this figure is small as compared with other neighbouring countries like Denmark (99%) the opening of the new Oslo airport has drawn great attention both from the government and the academic sector. Prior to its opening, the location of the Gardermoen Airport has been a major discussion issue in the Norwegian Parliament. The Parliament decided to locate the airport at Gardermoen delta, which is the largest unconfined aquifer in Norway. The new airport was established provided that its activities should not pollute the groundwater and the water balance within the aquifer and the surrounding water bodies (lakes and rivers) is maintained (28).

Potential contaminants from the airport are de-icing chemicals, jet fuel components and fire extinction chemicals (7). Propylene Glycol and Sodium Formate (formerly Potassium Acetate) are the main chemicals used for de-icing of runways and aeroplanes during the winter months (October-April). These chemicals are mixed with snow and start melting and infiltrating into the ground in early April.

Several questions has been raised and discussed concerning the fate of these chemicals and the major factors that govern their mobility in the subsurface. However in the last few years there have been significant changes in the groundwater chemistry of certain wells. The major changes occurred in two wells which showed increasing trend of Ca and Mg concentrations. This thesis is initiated to identify and describe the mechanisms behind these changes. The following sections will briefly discuss the background of the situation and present the results obtained from field data and laboratory works.

2. Background and Purpose

2.1 Geology of the Gardermoen Area

The Gardermoen delta is a raised, large ice contact deltaic complex deposited c 9500 years BP, during the early Holocene phase of the Scandinavian ice cap retreat [13, 34, 19 and 27]. It covers an area of 79km^2 and the geology is dominated by coarse gravel and sand sediments [29]. These sediments constitute the largest unconfined aquifer in Norway (Figure 2.1).

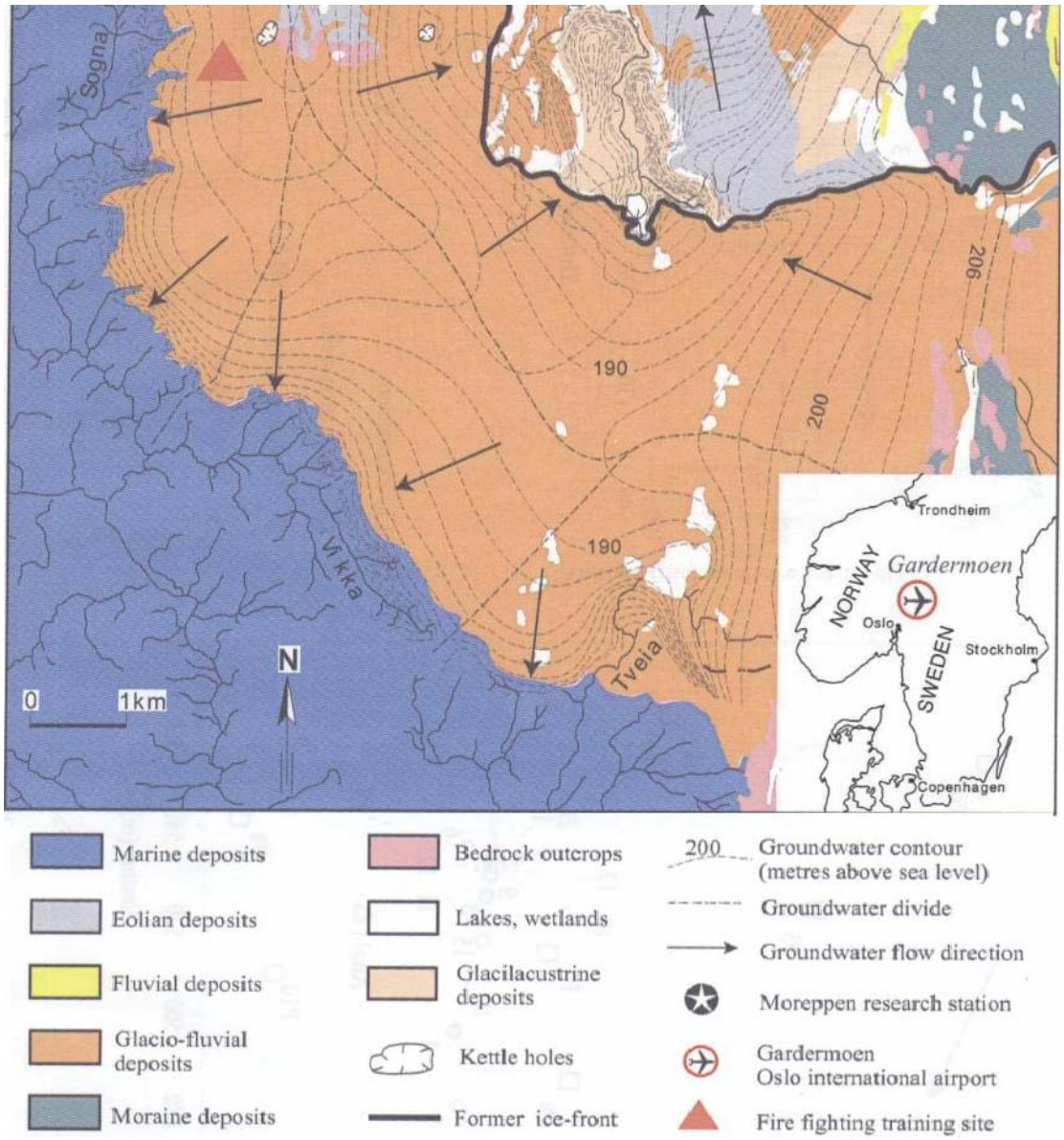

Figure 2.1 Location map and sediment cover of Gardermoen and its surroundings [29]

The delta was deposited in a shallow marine fjordal basin with an estimated water depth of less than 150m in a depositional time span of c. 70 years [29]. Borehole and

seismic data together with investigations on exposures were used to describe the extent and distribution of sedimentary facies and structures.

The sedimentary architecture of the Gardermoen delta complex consists of three units namely; (1) topset unit, (2) foreset unit and (3) bottomset units and is shown in figure 2.2 [29]. The thickness of these units varies with distance from the main glacier source, where the sediments are transported. These units are described briefly in the following sections.

2.1.1 Topset Unit

Boulder rich gravels, coarse sandy layers and pebbly sand layers characterize the topset unit. It consists of gravel beds dominated by cobbles intercalated with relatively thin and less extensive sand lenses. These sediments are distributed throughout the delta plain in varying thickness and extent. Depending on the distance from the main glacier source area, the thickness of the topset unit reaches up to 18m but generally thins to a meter or less in the delta front (Figure 2.2).

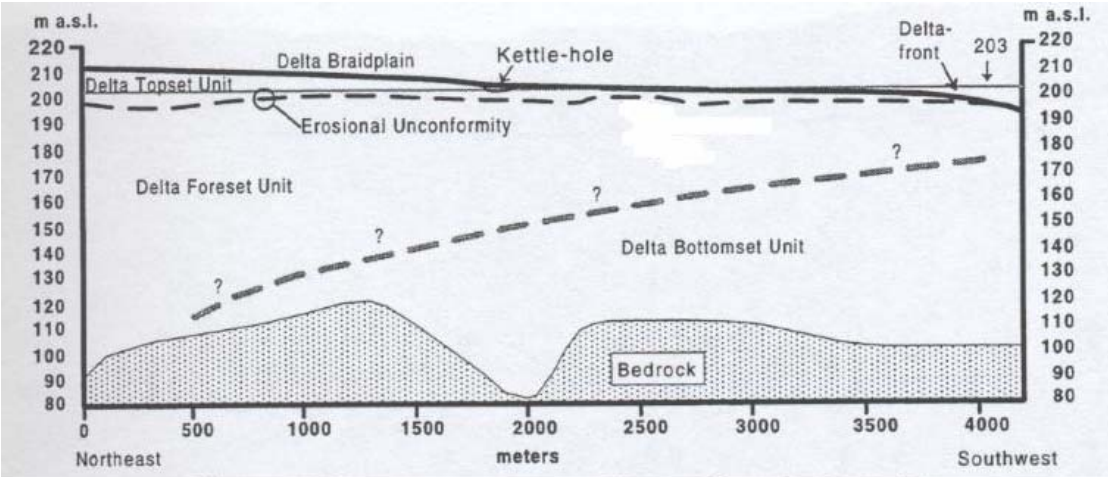

Figure 2.2 Vertical and horizontal extent of major units of Gardermoen delta

Boulder-rich gravels are common at the proximal zone, the zone nearest to the glaciers source. These gravel deposits are massive to crudely stratified structures. In the medial and distal zones (zones far from the main glacier source) the topset unit consists of finer sediments devoid of boulders. Sand facies dominate than gravels. Cross-stratified sand faces dominate in these zones [29].

The topset unit is generally well bedded and shows typical characteristics of river morphology of an outwash plain [29].

2.1.2 Foreset Unit

Parallel stratified sand layers constitute approximately 95 volume % of the exposed foreset deposits [29]. These layers are coarse to medium grained, with varying gravel content and generally dip into south.

The foreset unit also consists of massive sand and gravel beds ranging in geometry from lenses to chutes. The sand layers are coarse grained and contain pebbles and cobbles. Some gravel filled chutes occur in the proximal foreset zone of the delta plain. Silt and clay in the foreset unit are found in small quantity.

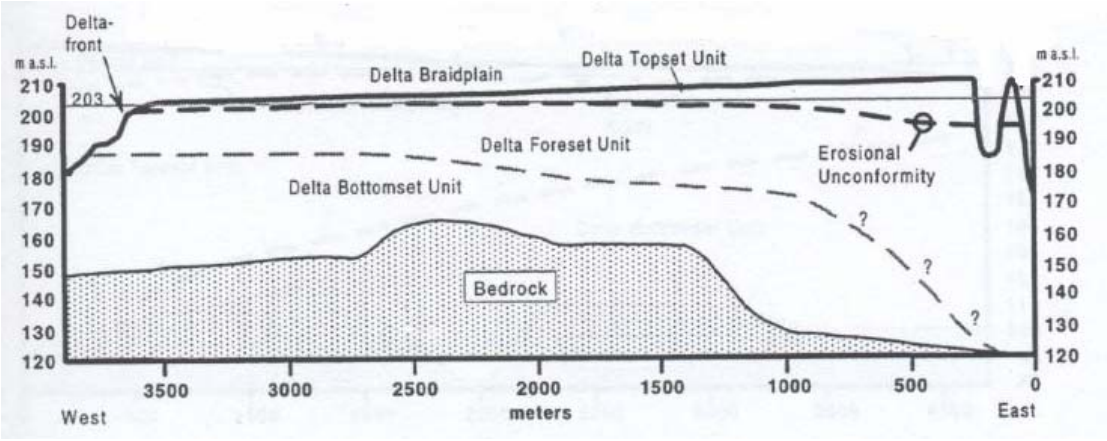

Figure 2.3 Cross-sectional view of the major sedimentary units at Gardermoen aquifer [29]

Variation of grain size from the proximal to the distal zones is not much pronounced as it is in topset unit. Ground penetrating radar (GPR) data from the upper surface at the Moreppen Research field shows southwest-dipping foreset beds in the east-west sections. The transition from the topset to the underlying bottomset unit is inferred to be at c. 15m depth [29].

2.1.3 Delta bottomset

Very few data was available from geotechnical drillings and cores from wells to describe the bottomset unit. Based on data from core recovered from Moreppen Research Field (Figure 2.1), the Bottomset unit consists of alternating layers of silt and fine sand. Silty clay sediments constitute the layers just above the bedrock, while the overlying sediments consist of thin layers of silt and very fine sands. Parallel-stratified, medium to fine sand layers are also observed interbedded with these sediments. The transition from the foreset to Bottomset unit lies between 15-20m as estimated from drillings conducted during the construction of the airport [29].

2.2 Hydrologic and Hydrogeologic setting of Gardermoen

2.2.1 Hydrology

During the International Hydrogeological Decade (1965-1974) a model was established for the Romerike area, which includes the Gardermoen delta [21,22]. Generally all the regional values for the hydrologic parameters of the study area are considered to represent the Gardermoen area although small local variations may occur.

The study area is characterized by flat catchment subjected to fairly uniform precipitation. The arithmetic average (1965-1974) for the annual precipitation was 794mm as measured during the decade. Half of the annual precipitation is lost due to evapotranspiration (400mm), which mainly occurs between May to September [15].

A major part of the precipitation is accumulated as a snow during winter mainly in November to March. The average snow accumulated for the 1968-1974 was 286mm [15]. The evaporation during the snow-melting period is close to 50mm leaving 236mm snow to melt and percolate through the soil profile and renew the groundwater. The snowmelt is due to rising air temperature and it normally takes 3 to 5 weeks duration.

2.2.2 Extent and aquifer characteristics

The Northern Romerike aquifer is an unconfined, precipitation recharged reservoir covering an area of approximately 105 km^2 [29]. The Gardermoen delta complex makes up 79km^2 of the Northern Romerike aquifer while glaciofluvial, glaciolacustrine and silty glaciomarine sediments made up the remaining part of the aquifer [29]. As discussed previously this delta complex is comprised of three units: topset, foreset and bottomset units.

Depth to the groundwater table ranges between 0 to 30 m below the surface. The groundwater table is located in the foreset delta unit. The saturated zone of the aquifer lies between the upper sandy foreset unit and the silty bottomset unit. In many of the kettle holes, springs and seepage surfaces of the groundwater table are seen on the surface.

The groundwater flows radially in two directions: north-northeast and south and west (Figure 2.1). River Risa and Lake Hersjøen are fed by the groundwater that flows to N-NE while Sogna and Vikka rivers drain the aquifer in south and west of the delta complex. The groundwater divide nearly divides the delta complex into two parts (Figure 2.1).

Tuttle (1997) suggested a Hydrogeological model that subdivides the saturated zone into three separate units. The lower unit (Figure 2.4) with hydraulic conductivity K value about 10^{-5} m/s and lower is found between the bedrock surface and the transition zone between the foreset and bottomset units. The intermediate unit has a hydraulic conductivity K value between 10^{-5} ~10^{-4} m/s and lies in the lower part of the foreset unit and upper part of the bottomset unit. Among all the units the upper unit has the highest K-value 10^{-3} to 10^{-4} m/s and mainly extends to the top of the delta foreset.

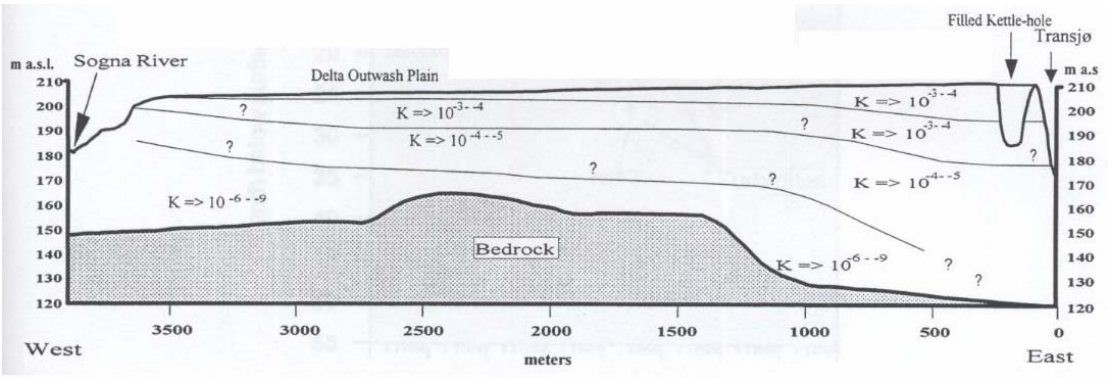

Figure 2.4 Hydrogeologic model of the aquifer [29]

The unsaturated zone consists of the delta topset which is slightly more permeable than underlying upper delta foreset unit. It is highly heterogeneous with alternating and tilting layers of varying texture [24].The thickness and extent of all the four hydrostratigraphic zones vary spatially throughout the aquifer complex. Note that the boundaries of these units do not coincide with the lithologic boundaries of the delta.

2.2.3 Groundwater Chemistry and Mineralogical Composition of Sediments

The Gardermoen aquifer is made up of glaciofluvial sediments which are predominantly comprised of gravel, sand and silt. Søvik (2001) described the mineralogical composition of soil samples taken from the upper 3m unsaturated zone at Moreppen Field station. Based on XRD analyses, these samples largely consist of quartz, K-feldspar, plagioclase, amphibole, chlorite and muscovite/Illite. Semi-quantitative description of the mineralogy of these soils revealed a general increasing trend of chlorite with increasing amount of silt.

Jorgensen (1990) also presented the XRD result of bulk samples collected from depths down to 50m. These samples have similar composition with respect to silicates (Table 2.1). Unweathered samples from nearby sites are found to contain calcite (2.4%) and pyrite (0.4-0.7 %).

Table 2.1 Summary of composition of sediments with respect to silicates (16)

Silicate Mineral	Weight (%)
Amphibolite	2
Chlorite	7
Biotite	2
Muscovite	13
K-feldspar	18
Plagioclase	8
Quartz	50

There are several lakes and rivers in the area which are recharged by the aquifer (Figure 2.1). The chemistry of these lakes and rivers is a direct reflection of the chemical composition of the groundwater. The average chemical composition of river Risa and the lakes in the study area are shown in table 2.3. These compositions were calculated on the basis of 31 analyses from each lake in which the samples were collected regularly during the IHD in the period 1967-1974 [22].

Important processes along the groundwater flow paths

The subsurface environment can be considered as a dynamic geochemical system consisting of (a) solid phase (minerals, amorphous solids and organic matter) (b) a soil gas phase and (c) aqueous solution phase [29]. The chemistry of groundwater evolved from major processes that involve the solid, gas and aqueous phases of the subsurface.

Rainwater is the source of most groundwater. It is dominated by oceanic vapour and it does resemble diluted seawater [1]. But natural and man-made dusts and gases modify its composition. Once rain water enters into the ground, various processes in the soil may affect the concentration. Dry deposition of dust particles and gases will dissolve. Evapotranspiration concentrates the solutes, and vegetation selects essential elements to store them temporarily in the biomass. Rock-water interactions like dissolution and precipitation of minerals will alter the chemistry of the rainwater until it reaches in equilibrium with all phases.

In the case of Gardermoen aquifer, the annual input-output budget of river Risa is used to determine the most important processes taking place along the groundwater flow paths. River Risa is almost entirely fed by groundwater and its chemistry reflects the groundwater composition. The input budget for this river and its catchment includes dry and wet deposition and is determined based on two years data from the Integrated Forest Study [14]. The hydrological budget, lake and river chemistry are taken from the data gathered during the IHD project (1967-1974) [23].

Table 2.2 Average chemical composition of the river Risa and the lakes (Modified from [16].

Lakes	pH	Conductivity (µS/cm)	Alkalinity (meq/l)	Concentration (mg/l)						
				Cl-	SO_4	NO_3	Na+	K+	Mg++	Ca++
1	5	13.54	0.01	0.9	3.65	0.02	0.54	0.37	0.29	0.65
2	5.48	11.94	0.01	0.85	2.77	0.12	0.53	0.49	0.37	0.75
3	6.73	29.7	0.26	1.13	3.66	0.12	1.41	0.46	0.81	3.73
4	7.59	187.8	1.88	2.75	14.83	0.36	2.8	1.65	2.69	37.88
5	7.68	226.9	2.38	4.61	14.12	0.1	4.93	1.47	3.9	45.56
6	7.21	161.6	1.16	4.7	29.45	0.27	3.4	1.53	3.31	28.7
7	5.45	35.2	0.03	1.44	11.6	0.12	1.45	0.48	1.02	4.06
8	7.77	254.5	2.61	6.19	18.3	0.11	5.77	1.51	4.65	50.94
Risa	7.71	171.6	1.6	2.86	12.1	0.11	3.12	1.24	2.86	31.39
Well*	7.93	201.5	1.91	1.14	14.87	0.02	1.91	1.25	2.53	39.08

1= Svenskestutjern, 2= Vibertjern, 3= Aurtjern, 4= Dragsjøen, 5= Mjøntjern, 6=Nordbytjern, 7=Sandtjern, 8=Transjøen
*Well- Deep Groundwater at Furusmo (30m)

Table 2.3 shows the average annual input and output budget. The values are divided by the total catchment area of river Risa and are given meq/m2 yr. As shown in the table, there is a large input-output difference for all major ions. This difference is mainly attributed to the major processes which are summarized below.

Table 2.3 Annual output-input budgets for river Risa [16]

Ion Species	Input		Output	Output-Input**
	wet	dry		
H^+	41.51	6.49	0.01	-47.99
Ca^{2+}	3.47	5.34	761.27	752.46
Mg^{2+}	2.06	2	114.31	110.25
Na^+	7.71	7.3	65.95	50.94
K^+	1.45	4.25	15.41	9.71
NH_4^+	21.87	5.03	0	-26.9
Cl^-	9.62	9.7	39.22	19.9
NO_3^-	24.13	8.22	0.87	-31.48
SO_4^{2-}	34.45	12.49	122.42	75.48
HCO_3^-	0	0	777.6	777.6

** Units are given by meq/ m2 yr

Leaching of Old seawater

The lower most part of Gardermoen aquifer was deposited under marine conditions hence fossil seawater is present in the sediments. The output for chloride, for example is higher than the input, indicating a contribution from leaching old seawater. By using the average composition of seawater it is found that the discharge from river Risa contains 2.61mg/l sea salt or 0.01 % fossil seawater [16].

Oxidation of Pyrite

Pyrite oxidation is a significant weathering process in unconfined sandy aquifer, which commonly results in stratified zones of aerobic iron rich and anaerobic pyrite containing zones in groundwater [18]. In the presence of oxygen pyrite containing sediments are oxidized to produce $Fe(OH)_3$ (s), SO_4^{2-} and H^+. Pyrite oxidation is one of the most important acid-producing reactions in geologic systems [5].

The output-input difference for SO_4^{2-} is 75.5 meq/l (Table 2.4). Oxidation of pyrite is the likely process that contributes to the difference because the sediments contain 0.4-0.7% pyrite. The major sediments that made up the aquifer are coarse-grained and there is high flow velocity that carries oxygen even to the deepest part of the aquifer. For instance the oxygen content of the groundwater from the deep groundwater well (Table 2.2) and a lake (1) is 0.5ml/l and 6.2 ml/l, respectively [16]. The oxidation of pyrite can be expressed by:

$$FeS_2 + H_2O + 3.5\ O_2 \leftrightarrow Fe^{2+} + 2H^+ + 2SO_4^{2-} \qquad (2.1)$$

Dissolved ferrous iron is unstable in the presence of oxygen but oxidizes to produce ferric hydroxide:

$$2Fe^{2+} + 5H_2O + 0.5\ O_2 \leftrightarrow 2Fe(OH)_3 + 4H^+ \qquad (2.2)$$

Equation (2.1) and (2.2) give:

$$2FeS_2 + 7H_2O + 7.5\ O_2 \leftrightarrow 2Fe(OH)_2 + 8H^+ + 4SO_4^{2-} \qquad (2.3)$$

The difference in oxygen content between deep groundwater and surface water is 5.7ml/l (0.25mmol/l). Using the annual water flux 486mm, the total oxygen consumption will be 121.5 mmol/m^3 /yr. According to Equation (2.3) oxidation of pyrite to form 75.5meq/m^3 SO_4^{2-} annually would require 70.8mmol/m^3 O_2. It was concluded that the observed reduction of oxygen in the groundwater is sufficient for the described pyrite oxidation.

Weathering and dissolution of carbonates and silicates

Weathering processes release elements to the groundwater. Carbonate weathering is responsible for large outputs of Ca^{2+}, Mg^{2+} and HCO_3^- while silicate weathering is the process behind Na^+ and K^+. Calcite weathering occurs simultaneously in three reactions:

$$CaCO_3 + H^+ \rightarrow Ca^{2+} + HCO_3- \quad (2.4)$$

$$CaCO_3 + H_2CO_3 \rightarrow Ca^{2+} + 2HCO_3^- \quad (2.5)$$

$$CaCO_3 + H_2O \rightarrow Ca^{2+} + HCO_3- + OH^- \quad (2.6)$$

The amount of annually formed bicarbonate is 775.5 meq/l (table 2.4); however the reactions in equation (2.4) and (2.6), where the pH increases from 5 to 7.7 only produce 4.86 meq/l. Consequently it was concluded that most of the calcite in the sediments is weathering following equation (2.5) [16].

Weathering of K-feldspar releases K^+ and HCO_3^- ions into solution by the following reaction:

$$2KAlSi_3O_8 + H_2O + 2H_2CO_3 \rightarrow 2K^+ + 2HCO_3- + Al_2Si_2O_5(OH)_4 + 4SiO_2 \quad (2.7)$$

Weathering of feldspar releases only 1meq HCO_3- for every mmol of H_2CO_3 consumed while for carbonate weathering (equation (2.5)) 2 meq of HCO_3- are released for each mole of H_2CO_3 consumed. The large output-input difference for HCO_3- is due to combined release of silicate and calcite weathering. This weathering is also responsible for differences seen in all major cations.

2.3 Airport Activity and Recent Changes in Groundwater Chemistry

2.3.1 Introduction

Norway is one of the countries in the world with long winter season characterized by snow falls. Like several airports in countries which have cold winter seasons, Gardermoen Airport has tackled the problem posed by snow and ice through different operational measures. De-icing is a critical and vital process to flight safety since even small amount of ice on the parts of the aircraft can impact its performance. Removal of snow from airfields and runways is also critical in maintaining continuous landing and take-offs. These removal and prevention measures require the use of various chemicals.

The most important activities of the airport that release chemicals to the subsurface environment are applications of de-icing chemicals on airplane surfaces and the runways in order to melt snow and ice during winter (Figure 2.5). Fire extinction chemicals and jet fuels are also potential contaminants which may be released to the environment by the airport.

Figure 2.5 Application of de-icing chemicals on airplanes

A variety of water-soluble inorganic salts and organic compounds are used to melt snow and ice from airplanes and runways. Commonly used de-icers include chlorides of Calcium, Magnesium and Sodium and organic compounds like Sodium Formate (HCOONa), Potassium Acetate (KAc) and propylene/ethylene glycols. These

chemicals are used in solid or liquid forms and frequently consist of additives like surfactant, pH buffer, corrosion inhibitor, flame retardant, or dye.

De-icing chemicals are preferred over one another based on their performance in melting, penetrating and disbanding snow from the applied surfaces and their corrosivity and environmental impact.

2.3.2 Chemical Principles of De-icing

Water containing dissolved substances always has a lower freezing point than pure water. Any soluble substance will have some de-icing properties. How far the freezing point of water is lowered by a solute depends only on the concentration, not on the nature of the dissolved particles. Given the same concentration of dissolved particles, the freezing point of water will be lowered the same amount by NaCl, $CaCl_2$, ethylene glycol or any other solute. This behaviour is called Colligative property [8].

The solubility of each de-icing substance at the final solution temperature determines how many particles can go into solution. This is the ultimate limit on the lowest freezing point attainable: ice will melt as long as the outdoor temperature is above the lowest freezing point of the solute-water mixture. Pure sodium chloride theoretically can melt ice at temperature as low as -6 ^{o}F, calcium chloride is effective down to -67^{o}F [8].

When a salt dissolves to form positive and negative ions, each ion counts as a dissolved particle. Ionic compounds such as sodium chloride (NaCl) and calcium chloride ($CaCl_2$) are efficient de-icers because they always dissociate into positive and negative ions upon dissolving forming more dissolved particles per mole than non-ionizing solutes. One NaCl molecule dissolves to form two particles, Na^+ and Cl^-; one $CaCl_2$ molecule forms three particles, one Ca^{2+} and two Cl^-, whereas the organic molecules ethylene/propylene glycols do not dissociate and dissolves as one particle. Three molecules of dissolved ethylene glycol are needed to lower the freezing point by the same amount as one molecule of calcium chloride.

Another advantage of calcium and magnesium chlorides is that they dissolve exothermically, releasing a significant amount of heat that further helps to melt snow and ice. Conversely, sodium chloride does not release heat upon dissolving. The dissolution of sodium chloride is slightly endothermic and has a small cooling effect. The difference in effectiveness for different de-icing chemicals is related primarily to their different solubilities at environmental temperatures, number of dissolved particles formed per pound of material, and exothermicity of dissolution [8].

The main advantage of organic de-icers, over their inorganic counters, is their lower corrosivity. Organic de-icers, such as calcium magnesium acetate (CMA) and ethylene glycol, are also said to be more effective than salts at breaking the bond between pavement and snow, allowing for easier ploughing and snow removal.

2.3.3 De-icing Chemicals used at Gardermoen Airport

Propylene glycol (PG) and sodium formate (formerly potassium acetate) are the main de-icing chemicals used at Gardermoen airport. PG is a colourless and viscous liquid at room temperature and is currently used for de-icing of airplanes. It can lower the freezing point of water to about -50^{o}C, depending on dilution. It is the major component of aircraft de-icers, making up 30 to 70% of the solution. PG is a neutral, weakly polar molecule, with a low octanol-water coefficient, which implies little adsorption to organic material [9]. It completely biodegrades under aerobic conditions but mercaptanes can be formed under anaerobic environments. Aerobic degradation takes the form:

$$CH_3\text{-}CH(OH)\text{-}CH_2(OH) + 4O_2 \longrightarrow 3CO_2 + 4H_2O \qquad (2.8)$$

This reaction involves formation of intermediate organic acids like lactic and pyruvic acid.

Sodium formate is a white, odourless and hygroscopic crystalline powder. It is soluble in water and readily dissociates into its ions as:

$$COOHNa \longrightarrow COOH^- + Na^+ \qquad (2.9)$$

This dissociation reaction increases the concentration of dissolved ions in the soil water. Cations in the percolating soil water may then interact with the soil particles through ion exchange mechanisms. Table 4 summarizes properties of PG and sodium formate/potassium acetate.

Table 2.4 Important properties of de-icing chemicals [9]

Deicing chemical	Molecular weight	Melting point(^{o}C)	Boiling point	Solubility	Density @20^{o}C	pH	BOD
PG	76.1	-59	188.2	-	1.04	-	2.2-57%
Sodium Formate	68.01	253	decomposes	0.97kg/l	1.92	7-8.5	-
Potassium Acetate	98.15	292	-	2kg/l	1.57	-	-

2.3.4 Biodegradation of Organic Compounds

Biodegradation is the breakdown of organic chemicals in soil through the activities of Microorganisms that are naturally present in soils. Biodegradation of organic compounds in soils depends on (i) susceptibility of the specific molecular structure of the organic compound to enzymatically catalysed chemical reaction (ii) the chemical and physical environment of the soil (temperature, Eh and pH) (21).

Biodegradation is an oxidation-reduction reaction since enzymes catalyse the transfer of electrons from the chemical that is being degraded to another chemical that accepts the electrons. The rate of the reaction will depend on the amount of both the electron donor and electron acceptor chemicals and on the amount of the enzyme/microbes present. The biodegradation rates of organic compounds are described by the help of Monod kinetic rate equation that is expressed as:

$$dS/dt = R_{Monod} = -k_{max} * S /(k_{1/2}+S) \qquad (2.10)$$

where S is the concentration of the organic compound (mg/l), t is time (s), k_{max} is the maximal rate (mg/L/s) and $k_{1/2}$ is the half-saturation constant. The half-saturation constant is defined as the rate of increase limiting concentration that allows the constituent to increase at half the maximum specific rate.

Organic compounds with polar functional groups (e.g. –OH, -COO e.t.c…) are more susceptible to microbial degradation because they are soluble in water and because microbes have enzyme that readily decompose such molecules (21). Both PG and sodium formate have polar functional groups and are soluble in water. Potential electron acceptors include dissolved oxygen under aerobic condition, and nitrate, iron, manganese and sulphate in anaerobic conditions.

2.3.5 Important processes in the subsurface

Gardermoen Airport covers a total 13 km^2 surface area and has two runways with a 3600 m and 2950 m long each (Figure 2.6). It has several square meters of impermeable surface that produce a large amount of runoff every year. Surface runoff from the airport contains deicing chemicals and hydrocarbons from jet fuel [4].

During the winter season (usually October to April) de-icing chemicals applied would be frozen and accumulate until the warm season arrives. As the snow starts to melt these chemicals would infiltrates and transported in the unsaturated zone. This is the time of year when the chemicals are likely to enter the groundwater [9].

The unsaturated zone at Gardermoen displays a complex heterogeneity of grain size distribution, hydraulic conductivity and other macro scale sedimentary structures [9]. These variations coupled with different degradation rates and micro organism population determine whether the deicing chemicals are degraded before reaching the groundwater. The main processes this contaminated water undergoes as it passes through the unsaturated zone include biodegradation, ion exchange reactions, and dissociation reactions. These processes are controlled by various factors that include for instance, pH, temperature and composition of sediments.

The groundwater chemistry is also affected as this water further percolates down and reaches the saturated zone. Data collected in the last eight years indicates an increasing trend of concentration of calcium and magnesium especially in two wells (Figure 2.6). Since 1997 several samples had been taken and analysed from wells in the airport and its vicinity.

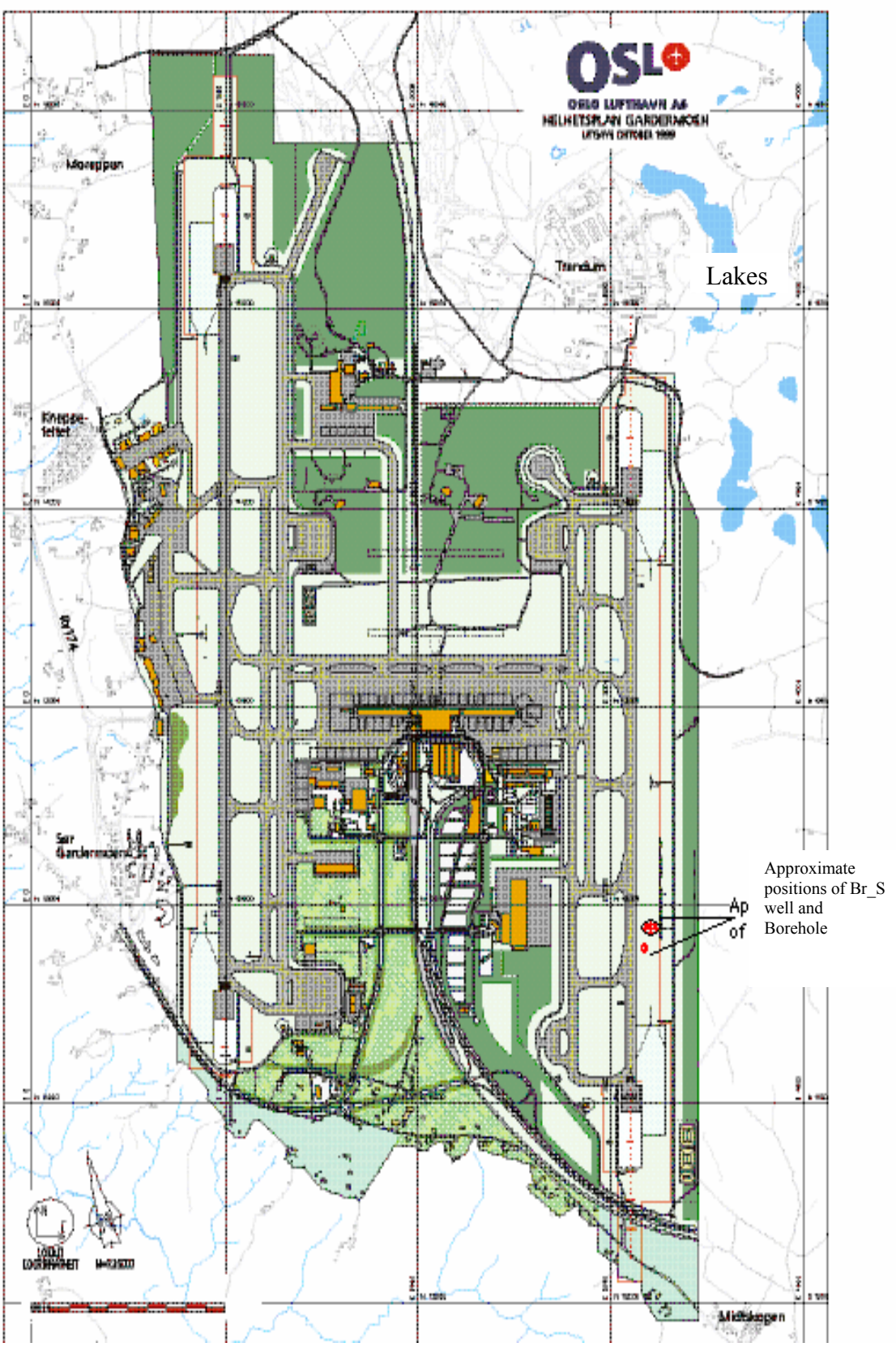

Figure 2.6 Gardermoen Airport and its surrounding (OSL)

Understanding the main reason behind these recent changes in groundwater composition is the basis for this thesis work. One possible mechanism that could lead to this increase is the exchange with calcium and magnesium on the soil surfaces.

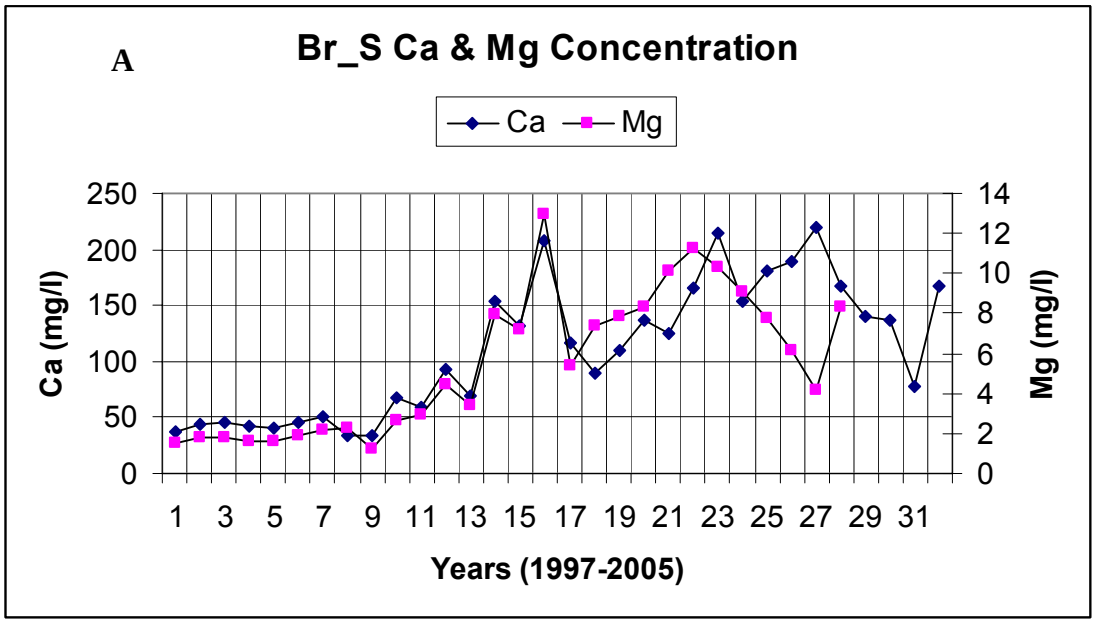

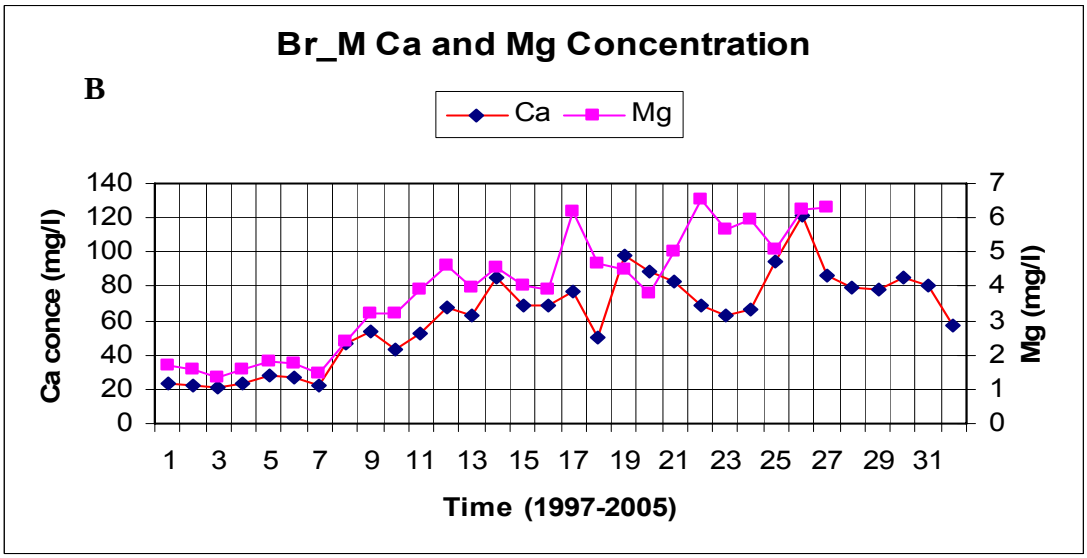

Figure 2.7 Variation of Ca and Mg concentration at Br_S (A) and Br_M (B) between 1997 to 2005 (Data points correspond to number of samples taken in those years)

2.4 Ion Exchange Capacity of Soils

2.4.1 Introduction

Soils are complex materials, reflecting the variability of the parent rock materials and organic residues from which they form. The elemental composition, mineralogy, chemical characteristics and morphology of soils is dependent on the physical and chemical properties of the parent material and the processes it was subjected to. Weathering processes, both physical and chemical, play a major role in the formation of soils and their properties. Physical weathering processes reduce the particle size of the mineral grains, increasing the exposed surface area. Chemical weathering processes will alter the rock forming minerals into secondary mineral products which are closer at equilibrium with the environment.

Inorganic material, organic matter, water and air are considered as the four major soil constituents [17]. Their amount may differ from soil to soil, or from horizon to horizon. The inorganic fraction of soils is derived from the weathering products of rocks and consists of rock fragments and minerals of varying size and composition. According to their size, the inorganic soil fractions are distinguished into three major groups: sand, silt and clay*.

Sand grains are chemically inert and do not carry any substantial electrical charges, hence have low water-holding capacity and exchange capacities. Their presence in soil promotes a loose and friable condition which allows rapid water and air movement. On the other hand clays constitute the smallest particles in soils and have colloidal properties. They carry electrical charges on their surfaces and are chemically the most active inorganic constituents in soils. Silts have somewhat intermediate size and chemical properties between clays and sands [17].

Chemical reactivity of soils is largely dependent on secondary mineral products and the amount of decomposed organic matter present. Ion exchange reactions are the most important chemical reactions involved in the interaction of soil particles with the soil fluid. Ion exchange is the reversible interchange of ions between a solid and a

liquid. Hydrated ions on a solid are exchanged, equivalent for equivalent, for hydrated ions in solution.

Oxides, clays and organic matter represent the finer materials of most soils. These particles have some specific characteristics, like net surface charges and large surface areas which enables them to determine the chemical reactivity of soils. The capacity of soils to exchange ions with the surrounding soil water is attributed to net charges on soil particles. Since the abundance of organic matter is confined to the upper layers of soil horizons, this section emphasizes more on secondary mineral products especially clays because of their abundance. Oxides and organic matter will be discussed briefly in later sections.

2.4.2 Clays

Clay minerals are generally considered to fall in the class of secondary minerals and derived as altered products of weathering of primary silicate materials such as feldspars and olivine. They are primarily layer silicates and constitute the major portion of the clay sized fraction of soils. Clays have a sheet-like lattice structure with either silicon in coordination with four oxygen atoms or aluminium in coordination with six oxygen atoms (Figure 2.8a).

Silica tetrahedral and Aluminium octahedral structures are the basic building blocks of clay minerals [13]. Clays are made up of alternating layers of tetrahedral (Si) and octahedral (Al) sheets (Figure 2.8a). The sheets are bonded together by the sharing of O^{2-} ions between the octahedral and tetrahedral cations [8].

* The term `clay` has various usages in soil literature. The clay fraction of soil includes all the soil particles with sizes less than 0.002 mm regardless of their composition. However, this term is also used to represent only clay minerals excluding oxides, organic matter and allophanes (amorphous clays). In this paper the latter usage is adopted.

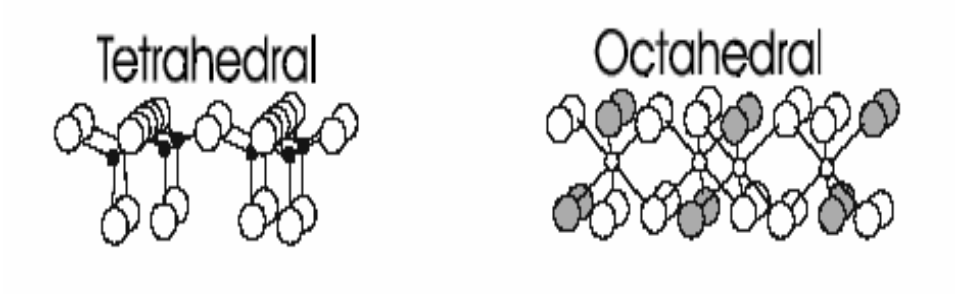

(a)

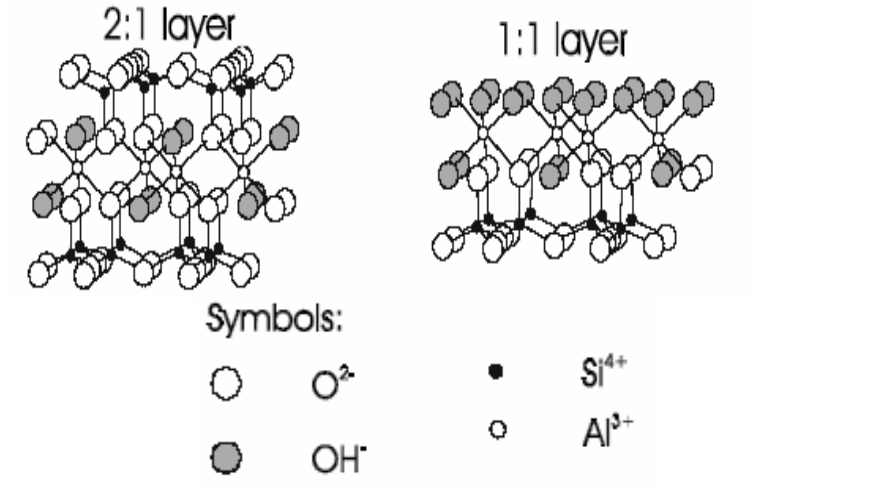

(b)

Figure 2.8 Structural units of clays (a) and their stacking (b)

The tetrahedral and octahedral sheets can be stacked on top of each other to form alternating layers. Classification of clays is mainly based on the type and number of sheets that form the layer. The superposition of one tetrahedral and one octahedral sheet result in a 1:1 layer. This layer type is represented in soils by the kaolin group, kaolinite being the most common mineral of the group (Figure 2.9). On the other hand, the superposition of two tetrahedral sheets with one octahedral sheet between them results in a 2:1 layer. There are three clay groups with the 2:1 structure: montmorillonite, illitic (mica), and vermiculite. Brief descriptions of the major clay groups are given below.

Kaolin group: This group consists of two main 1:1 clays, Kaolin and Halloysite. The two crystal units making up the 1:1 lattice are held together by hydrogen bonding between the OH^- groups of one layer and the O^{2-} ions of the adjacent layer and the interlayer space has a fixed dimension [17]. There is little isomorphic substitution in Kaolin and the CEC is largely from pH-dependent negative charges attributed to the

dissociation of protons from exposed OH groups. Halloysite, in contrast to Kaolin, contains water molecules in the interlayer space which resulted in high specific surface and CEC (Table 4).

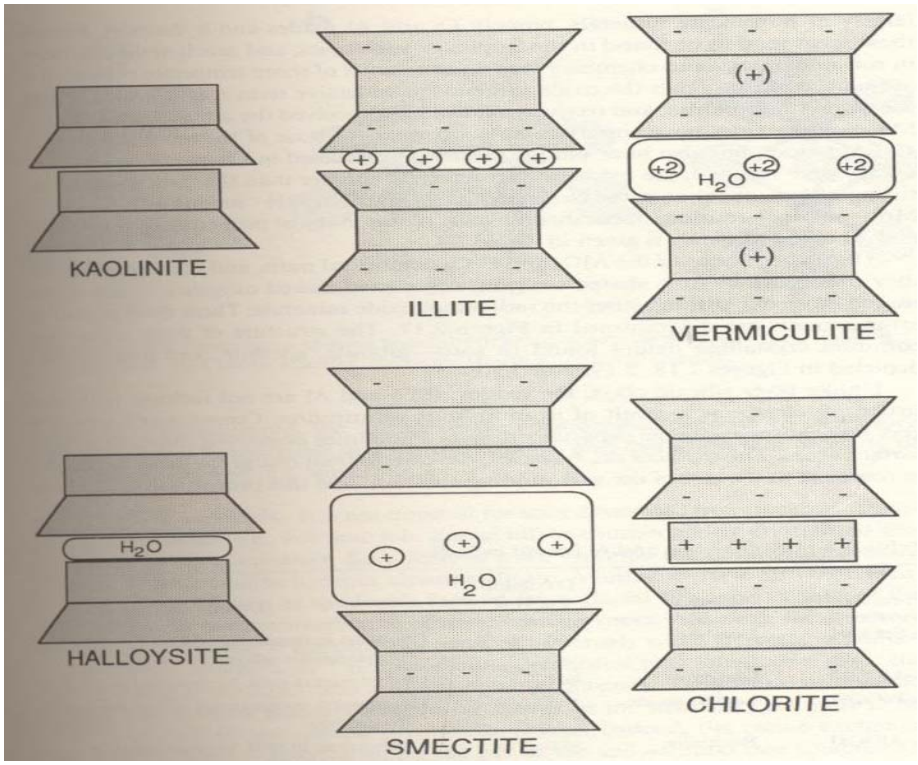

Figure 2.9 Common groups of silicate clays found in soils and distribution of charge and location of exchange cations, rectangles representing octahedral sheets and trapezoids for tetrahedral sheets [21]

Montmorillonite (Smectite) group: The crystal units making up the 2:1 structure in smectites are loosely bonded together by water in the interlayer space. This causes smectites to take on shrink-swell characteristics depending on soil moisture. The Al octahedral is heavily substituted giving rise to a more delocalized charge that allows water to penetrate between individual minerals and to adsorb cations on its internal and external surfaces [6].

Vermiculite groups: Like smectites, vermiculites have structures based on 2:1 lattice arrangements. They have a higher layer charge (and consequently a higher CEC) and do not swell in water as extensively as smectites.

Illite group: Illites are micaceous types of clays and variously identified as hydrous muscovite or hydromicas. They have similar structure to smectites but the interlayer

space is occupied by K^+ cations instead of water molecules. Hence Illite has less shrinking-swelling property than smectites.

Chlorite group: chlorites are often referred to as 2:1:1 clays since they are 2:1 clays with a hydroxide interlayer, either gibbsite or brucite [6]. They are hydrated Mg and Al silicates that are similar to mica minerals in appearance. They have very small charge and CEC because of the replacement of Mg^{2+} by Al^{3+} in the hydroxide interlayer [17]. They also have low specific surface areas because of the blockage of the interlayer regions by hydroxide sheets, and do not expand at all in water [6].

Table 2.5 Major types of clays and their important properties**

Clay types	Layer stacking	Specific surface (m^2/g)	Cation exchange capacity (mEq/100g)	Specific gravity
Kaolinite	1:1	10-20	3-15	2.60-2.68
Halloysite	1:1	35-70	5-40	2.00-2.20
Illite	2:1	65-100	10-40	2.6-3.00
Vermiculite	2:1	40-80	100-150	
Montmorillonite	2:1	700-840	80-150	2.35-2.70
Chlorite	2:1	80	10-40	2.6-2.96

** Modified from [21, 6]

Arrangement of alternating layers of tetrahedral and octahedral units strongly affects certain properties of clays, including 1) surface area 2) tendency to swell during hydration and cation exchange capacity [3]. Because of their small size clays exhibit large specific surface areas. The strong sorptive capacity of clays is derived from the negative charges created at the edges of these crystalline sheets where oxygen atoms have extra electrons that are not bonded to the cations in the crystalline structure. The negative charge can be further increased when ions with a lower valence substitute for ions with a higher valence in the sheet structure.

2.4.3 Oxides and hydroxides

Apart from clay minerals, oxides and hydroxides are the major non-silicate constituents of the clay fraction of soils. They are the principal portions of highly weathered tropical soils such as laterites and bauxites. The dominant oxides and hydroxides found in most soils are those of iron and aluminium, like hematite, goethite, gibbsite and boehmite [21].

Structurally, oxides are simpler than the layer silicates, consisting of hexagonal or cubic close-packed O^{2-} and/or OH^- anions with Fe^{3+}, Al^{3+}, Mn^{4+} or Mn^{3+} residing in octahedral sites [21]. With regard to ion exchange capacity, oxides and hydroxides do not develop permanent structural charges as a result of isomorphic substitution. In contrast to clay minerals they have very small ion exchange capacities even if they possess large surface areas. The mechanism of charge development on the surfaces of oxides and hydroxides is due to the fact that they are amphoteric (i.e. able to act as both acid and base) depending on the pH of the environment.

2.4.4 Organic matter

Soil organic matter originates from the decomposition of vegetation and animals, and occurs in soils in proportion as small as 0.5 to 5% by weight [32]. It is largely responsible for maintenance of good pore structure, retention of nutrients by cation exchange capacity and adsorption of potentially toxic organics [21]. Soil organic matter has high specific surface area (as great as 800-900 m^2/g) and a CEC that range from 150 to 300 cmol/kg. Thus the majority of soil surface CEC is in fact attributable to soil organic matter. It has been estimated that up to 80% of the CEC of soils is due to organic matter [17]. It is generally categorised into an unaltered debris and transformed products (humus) based on the state of degradation it undergo [21].

Humus is a complex material that has lost all the visible features of the organic residues from which it formed. It is further divided into amorphous materials which include all the humic substances and decayed materials (compounds that belong to recognizable classes such as lignins and polypeptides). Humic substances are divided

into humic (base soluble), fulvic acid (acid soluble) and humins (insoluble) according to their solubility in strong acid and base [21].

Soil organic matter has a greater variety of functional groups that control most of the properties of organic molecules and their reactions with other materials in the soil-water system. The most common functional groups are hydroxyls, carboxyls, phenolic and amines (Figure 2.10). The basic structure of all organics is formed by carbon bonds that are combined in saturated or non-saturated rings or chains as C and N combine with oxygen and hydrogen to form the various types of surface functional groups.

The functional groups can lose or gain hydrogen ions depending on the pH of the environment resulting in net negative or positive charges on soil surfaces. The carboxyls and phenolic OH groups contribute significantly to the cation exchange capacity of the soil organic material.

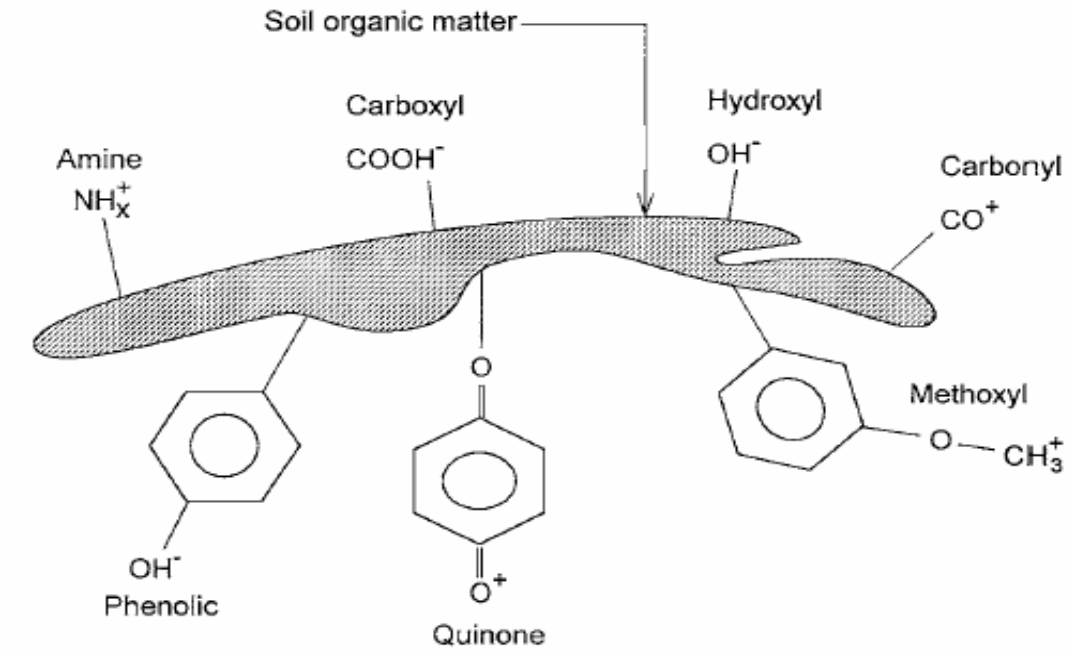

Figure 2.10 Typical organic matter and its functional groups (from [32])

2.4.5 Sources of surface charges on soil particles

Soil particles can acquire an electric charge in two main mechanisms. These two mechanisms are isomorphic substitutions and pH dependent chemical reactions.

2.4.5.1 Isomorphic substitution

Isomorphic substitution is a replacement of one atom by another of similar size in a crystal lattice without disrupting or changing the crystal structure of the mineral. It is very common phenomenon in clays and leads to charge imbalance in silicate clays which accounts for permanent charge on clay particles and for the ability of clays to attract ions to particle surfaces. It takes place during crystallization and is not subject to change afterwards. It takes places only between ions differing by less than about 10% to 15% in crystal radii. In silicate clays Al^{+3} cation may enter a lattice location intended for Si^{+4} or Mg^{+2} may substitute for Al^{+3}, resulting in a net negative charge on the crystal.

2.4.5.2 pH dependent charges

Chemical reactions dependent on pH may render net positive or negative charges to soil particle surface. Many solid surfaces (oxides, hydroxides and organics) contain ionisable functional groups such as –OH, -COOH, or –SH. At high pH, these groups lose H^+, becoming charged as $–O^-$, $-COO^-$, and $–S^-$. At low pH, these groups gain H^+, becoming $–OH_2$, $-COOH_2$, and $–SH_2$. At intermediate pH, the pH dependent surface charges may cancel each other and become zero and this pH is called the Point of Zero Charge (PZC) [21].

The relative magnitude of charges these mechanisms generate on soil particles is dependent on the type of materials and the chemical environment. In most clays the ion exchange properties are attributed to the permanent charges which result from isomorphic substitutions.

2.4.6 Types of Ion Exchange

Ion exchange includes both the exchanges of anions and cations with the solid surface. The cation exchange capacity (CEC) of groundwater is a function of the amount of inorganic clay minerals, oxides and organic humus present on the solid phase [31]. Materials coarser than clay size have smaller surface area and do not add significantly to the CEC.

Anion exchange may also occur on clay minerals, but to a much lesser extent than cation exchange because of the dominant fixed negative charge on the clay mineral surface. Displacement of hydroxide anions especially on broken edges of clay minerals favours anion exchange [17]. The anion exchange capacity (AEC) of clays is usually negligible at the pH of most natural material, but it can be on the order of 10% of the CEC for heavily weathered soils where conditions are relatively acidic [31].

2.4.7 Mechanisms of Ion Exchange

Groundwater consists of dissolved ions and its composition is a function of the sources and sinks of chemical elements along the groundwater flow path [31]. As water passes through soil, dissolved ions can leave the solution to become attached to oppositely charged sites on soil surfaces. This displaces ions of the same charge sign previously attached to the surface, so that they become dissolved and mobile in the water.

The selectivity of the ion exchanger (soil surface) for one ion over another can be explained using Coulomb's law which states 'for a given group of elements from the periodic table with the same valence, ions with the smallest radius will be preferred'. However ions in solution are surrounded by water molecules; therefore effective radius is the radius of the hydrated ion and not the bare ion. The larger the bare ion, the smaller the hydration radius; thus, for the group 1 elements the general order of selectivity would be $Cs^+ > Rb^+ > K^+ > Na^+ > Li^+ > H^+$ [6].

Because ion exchange is primarily an electrostatic process, the more highly charged solution species are preferentially adsorbed [31]. If ions of different valence are involved, generally the higher charged ion will be preferred. For instance, $Al^{3+}>Ca^{2+}>Mg^{2+}>K^{+}=NH^{4+}>Na^{+}$ [6].

This order of selectivity is called Lyotropic series and it assumes that ions are present at equal concentration in solution [31].

Another factor that affects the ion exchange mechanism is the concentration of individual ions in groundwater. Continual higher concentrations of any ion eventually displace most other ions having the same charge sign. For example, in typical Ca-HCO_3- groundwater Ca and Mg are the dominant ions in solution and their relative high concentration will result in their being more dominant ions on the exchange sites even though some other ions may be more strongly attracted to the exchange sites [31]. In contaminated groundwater where concentration of minor species could be high, the order of preference will follow the Lyotropic series.

The rate of ion exchange in soils is dependent on the type and quantity of inorganic and organic components and the charge and radius of the ion being considered. Generally, the rate of change decreases as the charge of the exchange species increases [6].

2.4.8 Quantification of Ion Exchange Mechanisms

The general term sorption includes all the processes that involve the transfer of mass between solid, liquid and gas phases of the subsurface environment. Ion exchange is one of these processes that involve replacement of one chemical (mostly ions) for another at the solid surface [1].

Ion exchange involves electrostatic interactions between a counter ion on a charged particle surface and counter ions in a diffuse (fluid) solution around the charged particle. It is usually rapid, diffusion controlled, reversible, and stoichiometric and in most cases there is some selectivity of one ion over another by the exchanging surface

[6]. Stoichiometry in ion exchange mechanisms means ions leaving the charged surface are replaced by an equivalent (in terms of ion charge) amount of other ions. This is due to the elecroneutrality requirement.

Although ion exchange is not a chemical reaction in the usual sense, the bonds broken and formed are long-range electrostatic bonds of low energy [21]. The exchange process is usually written as formal as that of chemical reaction.

2.4.9 Ion Exchange Equilibrium Constants

Several attempts have been made to define an equilibrium exchange constants for exchange processes and in this section only the most common ones are briefly discussed. These constants are often referred as selectivity coefficients rather than exchange constants since these values derived from these equations are not constants but vary as the composition of the solid surface changes [6].

For monovalent ion exchange, for instance Na for K, the reaction is written as:

$$Na^+ + K\text{-}X \leftrightarrow Na\text{-}X + K^+ \quad \ldots\ldots\ldots\ldots\ldots\ldots\ldots\ldots\ldots\ldots\ldots\ldots 2.11$$

where X represents the exchanger site. The equilibrium constant for equation x is given by:

$$K_{Na\backslash K} = (a_{Na\text{-}X})\,(a_K) / (a_{K\text{-}X})(a_{Na+}) \ldots\ldots \quad \ldots\ldots\ldots\ldots\ldots\ldots 2.12$$

Brackets represent activities of all species present in the reaction.

It is obvious that activities of dissolved solutes can be calculated from measured solution concentrations using the Debye-Huckel theory. For adsorbed species, however, there is no direct method to calculate the activities. This is because the activity of each exchangeable ion can be expressed as a fraction of the total, either as molar or equivalent fraction [1]. In addition to this the total number can be based on the number of exchange sites or on the number of exchangeable cations [1]. This is

the major difference among the conventions that are used to determine equilibrium constants for exchange processes.

The equivalent fraction (E) and molar fraction (M) of Na^+ in equation (2.12) can be determined from:

$$E_{Na} = \text{meq Na-X per kg soil/ CEC} \quad (2.13)$$

$$M_{Na} = \text{mmol Na-X per kg soil/ TEC} \quad (2.14)$$

where CEC is the cation exchange capacity of the soil in meq/kg of soil (in this case the sum of Na-X and K-X). Where as TEC is the total exchangeable cation, in mmol/kg of soil. For equations 2.13 and 2.14 both the CEC and TEC are the same because Na and K have the same valence hence all the conventions give the same result.

For ion exchange reactions involving hetrovalent cations the various conventions give significantly different results. For example for the exchange of Na for Ca, the reaction is written as:

$$Na^+ + ½\ Ca\text{-}X \leftrightarrow Na\text{-}X + ½\ Ca^{2+} \quad (2.15)$$

And the equilibrium constant as:

$$K_{Na\backslash Ca} = (Na\text{-}X)(Ca^{2+})^{0.5}/(Ca\text{-}X_2)^{0.5}(Na^+) \quad (2.16)$$

When the equivalent fraction of the exchangeable cation is used in the above equation it conforms to the Gaines-Thomas convention (K_{GT}) [10] whereas the Vanselow [30] convention (K_V) adopts the use of molar fractions. The activities of adsorbed ions are expressed in terms of the total exchangeable ions in both of these conventions.

On the other hand, if the activities are expressed as a fraction of the number of exchange sites (X-), the reaction in equation (2.15) takes the form:

$$Na^{+} + Ca_{0.5}\text{-}X \leftrightarrow Na\text{-}X + 0.5Ca^{2+} \qquad (2.17)$$

With $K_{Na\backslash Ca} = (Na\text{-}X)(Ca^{2+})^{0.5}/(Ca_{0.5}\text{-}X)(Na^{+}) = E_{Na}\,(Ca^{2+})^{0.5}/E_{Ca}(Na^{+})$…..

Equation (2.17) gives the Gapon Convention (K_G) [11] in which the molar and equivalent fractions are the same because both are based on a single exchange site with charge -1.

3. Materials and methods

Field data supplemented by laboratory experiments form the basis of understanding the major mechanisms that govern the problem under consideration. In this thesis, the main issue is to understand the effect of ion exchange processes in altering the composition of groundwater at Gardermoen aquifer. The Airport has monitored the aquifer using several of the monitoring stations and wells installed to collect snow water and soil samples. These samples are frequently gathered and analysed with regard to quality of the groundwater and are widely used in this work.

In addition to these, geochemical modelling using the PHREEQC-2 code has been conducted to strengthen the findings from the field and laboratory works.

3.1 Field Samples

3.1.1 Water Samples

One of the major activities conducted during the establishment of Gardermoen Airport was the installation of monitoring wells to follow-up the effect of chemicals discharged to the ground. The Airport periodically conducts sampling of groundwater and snow fall. Chemical analysis of these water samples are used to identify any change that occurred in the groundwater over a period of time.

In this thesis water and snow samples collected since 1997 are used. These samples are analysed with respect to major cations, dissolved organic components and physical properties. The snow samples used comprise recent data that are taken in winter season of 2006. Complete record of the water samples is given in Annex VI.

3.1.2 Soil Samples

Seven soil samples were taken from a well drilled 10m NE of Br_S (Figure 3.1). Each of these samples represent 1m thick soil profile including the unsaturated and saturated zones, these samples cover a total of 19m thick soil profile (Figure 3.2).

3.2 Laboratory Experiments

3.2.1 Grain size Analysis

Grain size analysis of the soil samples is conducted in Jordforsk Laboratory in the agricultural University of Norway (Ås). Fractions of the major sizes for each sample are tabulated and only a summary of the analysis done is used in this work.

3.2.2 Mineralogical Composition by XRD method

Mineralogical composition of these soils was determined by an X-ray diffraction method. Powder XRD analysis was carried out on a Philip's X'pert X-ray diffractometer (Philips, Eindhoven, the Netherlands) equipped with θ-θ goniometer and Cu-Kα radiation.

3.2.3 Carbon Analysis

Total carbon (TC) content and total organic carbon (TOC) content were analysed using a CR-412 Carbon Analyser which measures CO_2 release after thermal oxidation. This uncertainty involved in this method is approximately 0.03%. The total inorganic carbon (TIC) is given as a difference of TC and TOC.

3.2.4 Exchangeable cations and Cation Exchange Capacity

Cation Exchange Capacity (CEC) is the measure of a soil to retain readily exchangeable cations which neutralize the negative charges of soils. There are several conventional methods for CEC analysis in which most of them involve saturation of the soil sample with a known solution and displacement of exchangeable ions. Ammonium nitrate and Strontium chloride solutions are used to measure the CEC of the soil samples in this work.

After drying the samples at 30^oC in an oven, the samples are sieved through 2mm sieve. Sufficient amount of 1M NH_4NO_3 solution is added to 25g soil from each sample and the mixture left for overnight on shaking machine in order to achieve

sufficient saturation of the soil. The sample is then filtered into 250ml flask and repeatedly washed by 1M NH_4NO_3 to make a total extract of 250ml.

Concentrations of major ions (Ca^{2+}, Mg^{2+}, Na^{+}, K^{+}, Fe^{2+} and Al^{3+}) in the extracts were quantified as the sum of total free ions and by Atomic Absorption Spectrometer (AAS, Varian SpectrAA-300, Varian Techtron, Springvale, Australia) using a three point standard calibration curve. The concentration range of the standards was varied depending on the concentration of the ion of interest. The instrument gives the concentration values in mg/l. The procedure is given in Annex II CEC determination procedure.

The CEC of the soil samples is also analysed using Strontium Chloride ($SrCl_2$) solution. Instead of a shaking machine, a centrifuge is used in this case. The sample is then washed by alcohol and distilled water before it is dried at $60^{o}C$ in an oven. A powder is prepared from the dried sample and mixed with SpectroFlux in 1:9 ratios. This mixture is melted at $1150^{o}C$ in machine in order to get colourless beads for quantitative X-ray fluorescence analysis.

3.3 Geochemical Modelling

Modelling of the PHREEQC-2 is a computer programme designed to simulate the diverse hydro geochemical reactions and transport mechanisms in both natural and polluted waters [24]. It is capable of simulating 1-D transport and thermodynamic equilibrium including ion exchange, dissolution and precipitation of minerals.

PHREEQC includes ion exchange in the form of association half reaction with constraint that the exchanger is always fully occupied by ions i.e. no free X- ions exist [2]. In the database of PHREEQC, cation exchange is defined according to the Gaines-Thomas convention (1953). PHREEQC handles exchange reactions by splitting them into half reactions in which the corresponding association constants are given relative to $K_{Na\backslash X}$ where the Na\X subscript is the exchange of Na^{+} ions with X ion [1].

3.3.1 Site Description and Computer Code

Modelling conducted in this thesis refers to a well drilled near the eastern runway of the international Oslo Airport (Figure 2.1). All the soil samples taken from this well are dominantly made up of medium to fine grained sandy soils, the fine portion increasing with depth (well log provided in Annex I). The groundwater table is at 13.8m depth.

The well is represented by 22m length column with specific cells given CEC values found from analysis of soil samples (Figure 3.1). The groundwater composition from nearby well is used to represent the pore water solution. Chemical composition of snow samples containing de-icing chemicals are used as influent solution. The CEC values are entered after being converted into meq/l of pore water. The input file for the column modelling is given in Annex IV.

Three types of discretizations were conducted; 22, 44 and 88 cells with 1, 0.5 and 0.25 meters length each respectively. The grids are refined to check the behaviour of the model. The parameters used in the transport simulation are shown in Table.

Besides cation exchange reactions, it is also tried to model the behaviour of biodegradation of Formate in the subsurface using Monod kinetic rate equation (Equation 2.10). This rate equation can be modelled in PHREEQC by defining parameter values for the half saturation constant ($k_{1/2}$) and the maximal growth rate (k_{max}.) (Annex VII).

3.3.2 Model Assumptions

The modelling performed in this thesis emphasizes on understanding the contribution of cation exchange processes to the recent increase of Ca^{2+} and Mg^{2+} in the groundwater. Consequently, all other major processes, which otherwise could have significant influence on the results from the model are kept to be constant in the simulated column. Aquifer sediments are also considered to be homogeneous with respect to porosity, sedimentary structure and other physical properties.

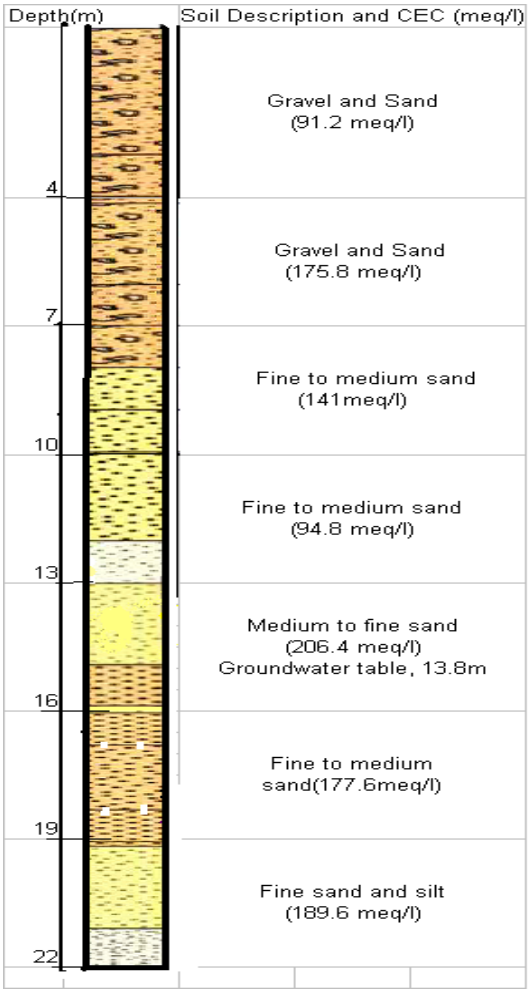

Figure 3.1 Column representation of the modelling

Composition of the influent solution is recalculated from snow samples analysed for major de-icing chemicals used. Propylene glycol (PG) and sodium formate together with other additives are the principal de-icers widely used at the airport. Snow collected from nearby site from the modelling site is used as influent solution (Annex III).

Propylene Glycol is a weakly polar, soluble compound and it does not have much effect on cation exchange processes. Sodium formate, on the other hand, readily dissolves in water and yields free Na^+ ions available for cation exchange. CEC values obtained from the seven samples are also converted into mmol/kg of water units and entered in the model after averaging the values over depth.

Biodegradation parameters in this modelling are adopted from literature data because they are difficult to obtain for field conditions and are usually a subject to large uncertainties and spatial variabilities (20).

4. Results and Discussion

4.1 Mineralogical Composition and Grain size Analysis

Grain size analysis of the soil samples was conducted at Jordforsk Laboratory at Agricultural University of Norway (Ås). Only the results are summarized and presented here. As shown in table 4.1, except for samples 6 and 7, which contain more than 40% gravel all the samples predominantly consist of sand. The silt fraction of the samples increases with increasing depth.

Table 4.1 Grain size analysis result of the samples

Soil Type	Grain Size(mm)	Sample Number						
		6	7	8	9	10	11	12
Gravel	Coarse (20-60)	3.8	0	0	0	0	0	0
	medium(6-20)	16.3	15.8	0.1	0.1	0.8	0	0
	fine(2-6)	25.4	25	0.8	0.3	2.3	0.2	0.1
Sand	coarse(0.6-2)	31.4	27.6	2.5	2.9	10.1	5.8	1.1
	medium(0.2-0.6)	15.3	23	31.9	42.3	57.5	51.3	24.8
	fine(0.06-0.2)	4.7	5.9	60.4	43.9	27.3	38.1	59.5
Silt	<0.06	3.1	2.7	4.3	10.6	1.9	4.6	14.5

Mineralogical composition of the soil samples was carried out by the help of X-ray diffraction method. Calcite is identified in only one sample (Sample No 10).Quartz, amphibole, K-feldspar, Plagioclase and few clay minerals mainly Illite and muscovite peaks are identified on the samples (Table 4.2). This result is very similar to the one discussed in previous sections (Section 2.2.3). The major minerals qualitatively identified in the samples are given in Annex V.

Table 4.2 Major minerals identified in soil samples

Minerals Identified	Sample Number						
	6	7	8	9	10	11	12
Quartz	x	x	x	x	x	x	x
Albite	x	x	x	x	x	x	x
Muscovite	x	x	x	x	x		
Sanidine	x						
Clinochlore	x	x		x	x	x	x
Magnesiosadanagaite	x	x					
Microcline	x	x	x	x	x		x
Illite		x	x			x	x
Orthoclase		x					
Calcite					x		

4.2 Cation Exchange Capacity

Measured cation exchange capacity (CEC) values obtained from Ammonium Nitrate and Strontium Chloride methods are shown in Table 4.3 and Figure 4.1. Both methods give fairly similar results except for samples 7 and 9, which show large discrepancies (32 and 57 %). Generally sandy soils exhibit low CEC usually less than 4 meq/l.

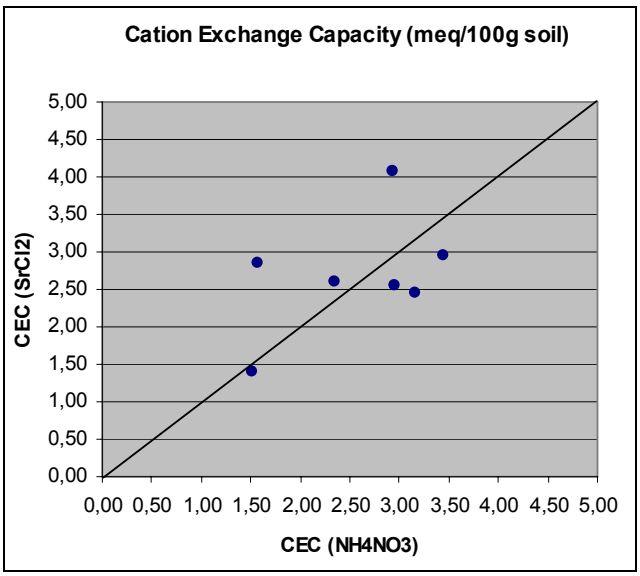

Figure 4.1 Comparison of CEC results from NH_4NO_3 and $SrCl_2$ methods

Table 4.3 CEC result from NH_4NO_3 and $SrCl_2$

Soil Samples	Depth(m)	CEC (meq/100g)	
		NH_4NO_3	$SrCl_2$
6	3.5	1.52	1.40
7	6.5	2.93	4.08
8	9.5	2.35	2.60
9	12.5	1.58	2.86
10	15.5	3.44	2.96
11	18.5	2.96	2.56
12	21.5	3.16	2.44

As shown in Figure 4.2 the CEC of soils has increased with depth. This is based on the fact that the amount of fine sand and silt increases with depth. Grain size is an important factor in determining CEC. These sediments have large surface areas and have large CEC values (section Cation Exchange Capacity). Sample 10, which is fine sand, has the highest CEC (3.44meq/100g), while sample 6, which is coarse sand to gravel, has the lowest CEC (1.52meq/100g).

Apart the relationship of CEC to depth, an interesting contrast is seen among the samples. Soils samples obtained from the part of the aquifer below the groundwater

table, which is 13.8 m (samples 10, 11 and 12) have significantly higher CEC value than those taken from the unsaturated zone. The three samples only contribute 53.3% of the total CEC from all samples. Groundwater contains dissolved ions that are involved in exchange or any processes that ultimately affect the soil composition.

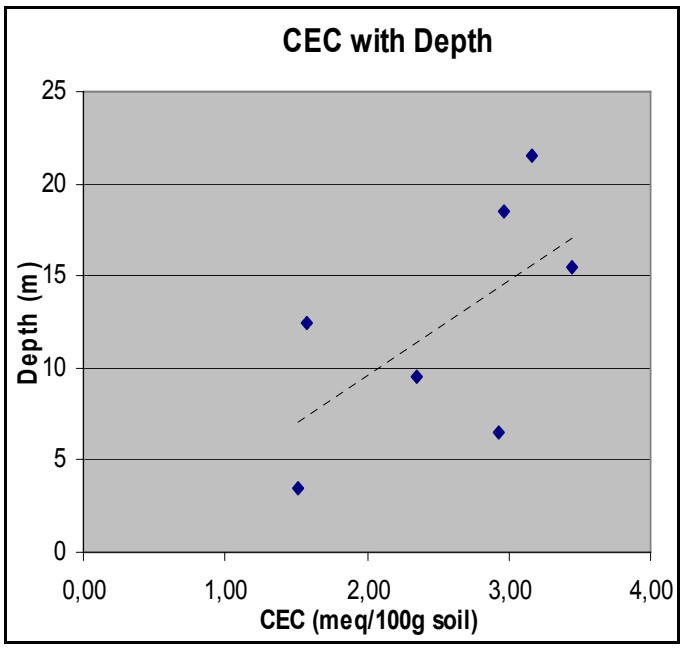

Figure 4.2 Variation of CEC with depth

The relationship between Total Inorganic Carbon (TIC) and CEC is shown in Figure 4.4. TIC varies as similar as the CEC following the same trend, soil samples that have small CEC values also display small TIC.

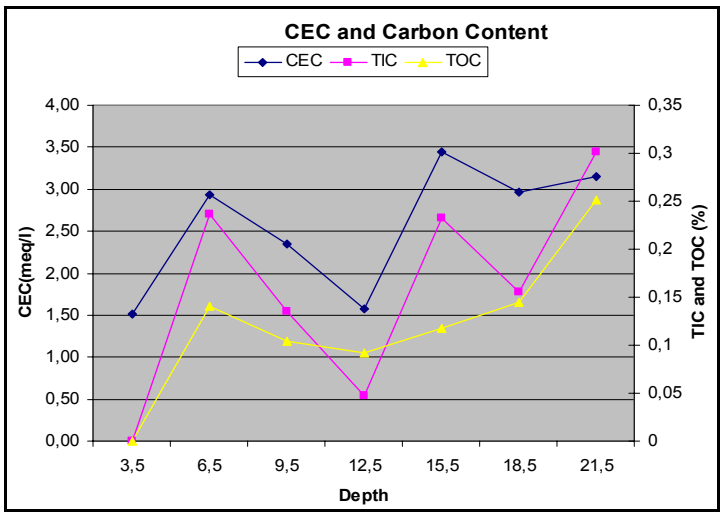

Figure 4.3 CEC with total carbon (TC) and total inorganic carbon (TIC)

Equivalent fractions of the major cations on soil surface are plotted to determine the most dominant cation on the soil exchangers (Figure 4.4). Calcium and magnesium occupy nearly 90% of all the exchange sites available. The fractions of major cations are given in Table 4.4. The fraction of Calcium in all samples is higher than the combined sum of the remaining cations.

Table 4.4 Equivalent fractions of major cations on exchange sites

Sample	CEC	β_{Ca}	β_{Mg}	β_{Na}	β_{K}
6	1,52	0,69	0,20	0,025	0,069
7	2,93	0,85	0,11	0,011	0,025
8	2,35	0,88	0,08	0,007	0,025
9	1,58	0,74	0,20	0,009	0,039
10	3,44	0,91	0,05	0,014	0,015
11	2,96	0,93	0,05	0,006	0,016
12	3,16	0,90	0,07	0,005	0,020

Without the presence of Na and K, the equivalent fraction of Ca and Mg would follow the ideal line (dotted line figure 4.4). The effect of Na and K is clearly seen by lowering the ideal exchange line by factors related to their equivalent fractions.

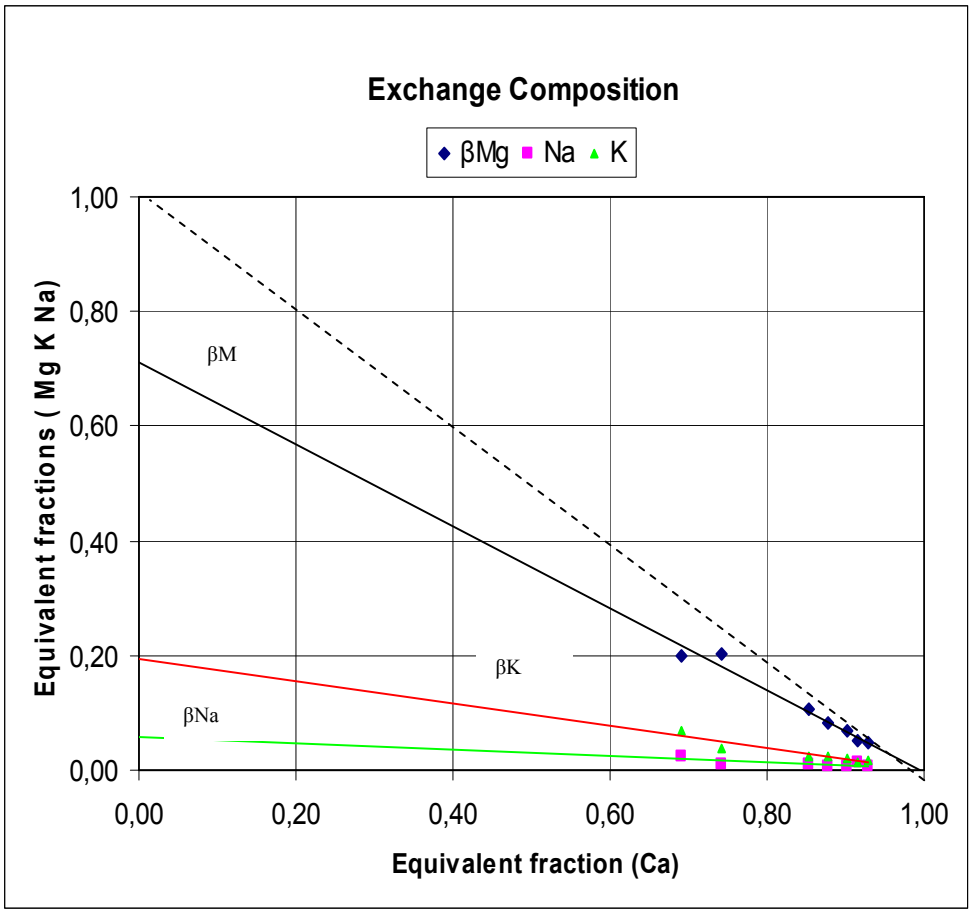

Figure 4.4 Equivalent fractions of Na, Mg and K plotted against Ca

4.3 Modelling Result

Numerical modelling was conducted to simulate the field using three discrete column grids. All the three discretizations gave the same result clearly indicating the model behaves well. Hence only result from one column grid is presented here. The average velocity of groundwater in the study area that includes the Gardermoen aquifer is between 0.1-0.2m/day [15]. Taking into account the velocity the time step used in the simulation is 617143 seconds (7.14 days). As shown in Figure 4.5 both the concentration of Ca and Mg rise while the free Na+ cation and formate anion concentration in the pore solution falls. The concentration of K is not much affected.

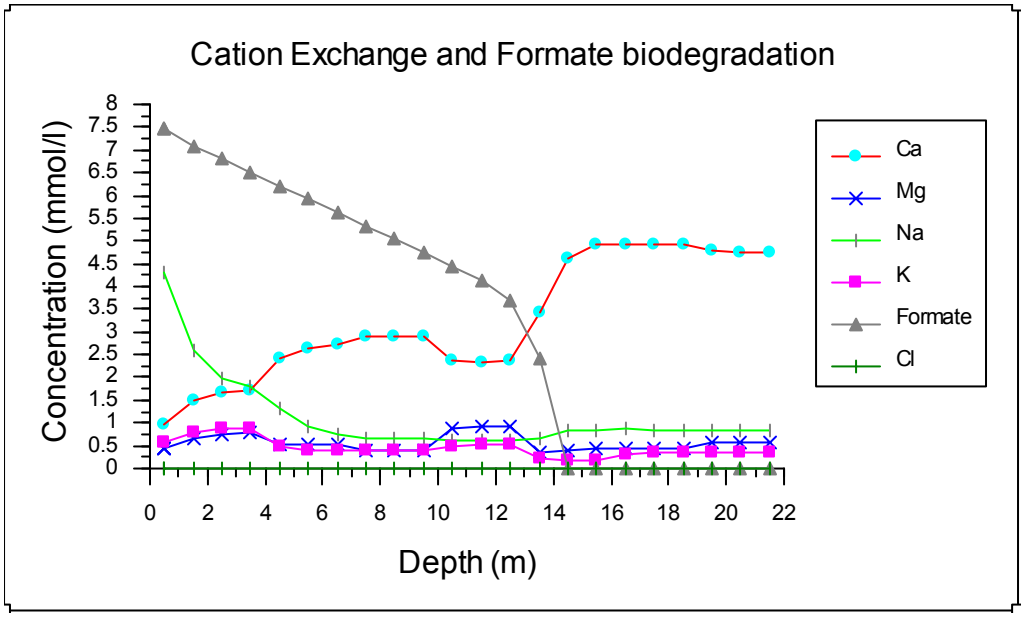

Figure 4.5 Cation exchange and formate biodegradation from PHREEQC-2

Biodegradation of formate in a batch experiment is displayed in figure 4.6. The Monod rate reaction employed in the model used two specific values for the half saturation constant and the maximal growth. Over the period of 60 days formate showed visible biodegradation. It reaches half of its original amount between 20-28 days.

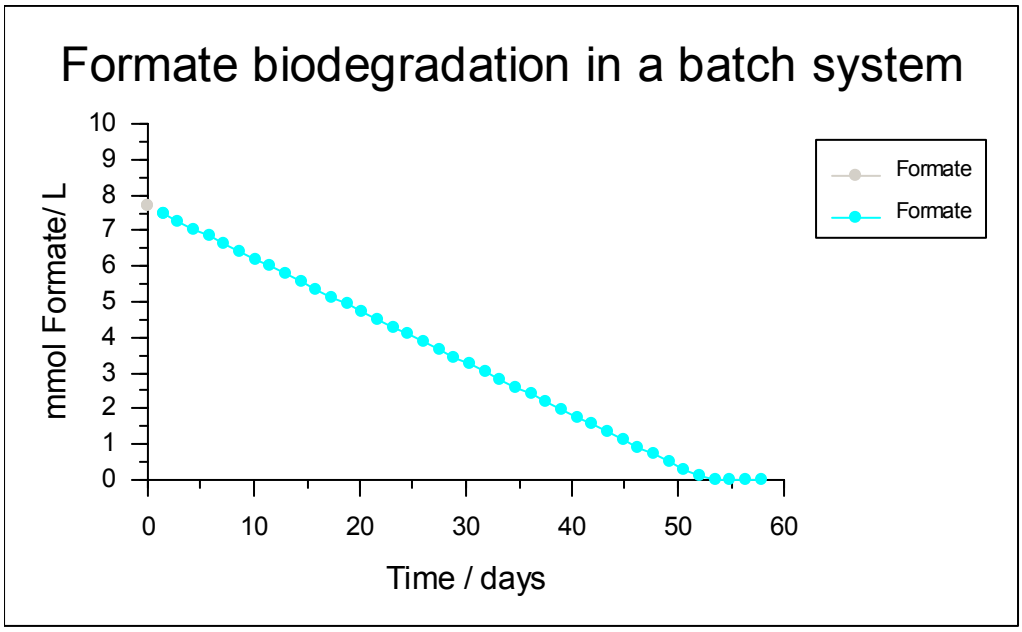

Figure 4.6 Biodegradation of formate in a batch system

5. Conclusions and Recommendations

It has been discussed in the previous sections that introduction of de-icing chemicals into the subsurface could cause significant change in the chemistry of the groundwater. The processes responsible for these changes may include ion exchange reactions, biodegradations and dissociation reactions. Some of these processes involve intermediate and final degradation products like carbonic acid and bicarbonates. These compounds increase the dissolving power of the groundwater as it passes through the soil particles. This leads to dissolution of minerals which subsequently increase the concentration of important ions in the groundwater.

Large amount of Na^+ and K^+ cations is available due to the dissociation of Sodium formate (formerly potassium acetate). As long as the use of these chemicals continue in the airport there will always a continuous supply of these ions into the groundwater. These ions readily exchange with cations on the soil particle surfaces and give an increase in Ca^{++} and Mg^{++} in the groundwater.

Based on the data gathered and subsequent laboratory works and computer modelling the following conclusions are drawn:

1) The equivalent fraction of Calcium in all samples is high as compared to other cations suggesting that it is the major ion that readily exchanges with Na^+ ions in groundwater. This conclusion is consistent with the result obtained from groundwater samples of the two wells (Br_S and Br_M) discussed in section 2.3.4.

2) The CEC values obtained for the soil samples are generally acceptable for sandy soils, which are expected to be at the lower range as compared to clays and organic matter. However since groundwater is in constant motion (especially in sandy aquifers like Gardermoen delta) it will interact with more cation exchange sites. Hence the Na^+ concentration in the groundwater will be buffered even in very small CEC values.

3) The concentration of Na^+ in the groundwater is far higher than any of the cations on the soil exchanger; hence concentration will be the governing factor in ion exchange processes than the effects of higher charge and hydration radius.

4) The increasing trend of Ca^{++} and Mg^{++} concentrations in the groundwater will continue as long as there is sufficient of these ions on the soil exchanger. However, the question about how large is the supply of CaX_2 and MgX_2 is still unresolved. Determination of this quantity requires advanced approach that will characterize the rate of dissolution and precipitation of minerals and weathering processes and by-products.

Degradation of Propylene glycol involves the production of intermediate organic acids. These acids lower the pH of the pore solution ultimately increasing its dissolving power. Additional research on the fate and transport of propylene glycol and sodium formate is necessary in order to describe the actual field condition.

The effect of redox reactions, dissolution and precipitation of minerals, biodegradation processes is not addressed in the present thesis. Further studies directed on understanding these processes and their influence on the groundwater composition will give a better explanation of the changes seen.

The quality and accuracy of the geochemical modelling conducted in this thesis can be improved if additional data are available. These data include composition of pore water solution in the unsaturated zone, accurate parameters and representative rates of degradation for the chemicals involved.

6. References

1. Appelo, C.A.J and Postma, D., 2005. Geochemistry, groundwater and pollution 2nd edition A.A.Balkema Publishers Amsterdam Netherlands

2. Appelo, C.A.J and Willemsen, A,. 1987. Geochemical calculations and observations on salt intrusions 1. A combinedgeochemical/mixing cell model. J. Hydrol., 94:313-330

3. Boulding, J.R and Ginn, J.S Practical handbook of soil, vadose zone and groundwater contamination: assessment, prevention and remediation 2nd edition, CRC Press/Lewis publishers Retrieved 22/01/06 from www.EnviroNetBase.com//books/1150/L1610C01.pdf

4. Breedveld, G.D., 1996. Treatment of Jet fuel contaminated run-off water by subsurface infiltration; paper submitted to the Proceedings to the Jens Olaf Englund Seminar "Protection of groundwater resources against contaminants" Edited by Per Aagaard and K.J. Tuttle Gardermoen Norway

5. Domenico, P.A. and Schwartz, F.W., 1997. Physical and Chemical Hydrogeology 2nd edition John Wiley and Sons Inc. New York

6. Donald, L.S., 1995 Environmental Soil Chemistry, Academic Press San Diego

7. Englund, J.-O., Moseid, T., 1992. Introductory Report. Literature Review and project catalogue. Oslo. The Norwegian National Committee for Hydrology. The environment of the subsurface, Part I: The Gardermoen Project, 1992-94

8. Eugene, R.W, Application of environmental chemistry: a practical guide for environmental professionals, CRC Press 2000. Retrieved 22/01/06 from http://www.environetbase.com//books/1911/L1354_ch06.pdf

9. French, H.K., 1999 Transport and degradation of de-icing chemicals in a Heterogeneous Unsaturated Soil, Ph.D thesis, Agricultural University of Norway, Ås

10. Gaines, G.L. and Thomas, H.C., 1953 Adsorption studies on clay minerals. II. A formulation of the thermodynamics of exchange adsorption. J.Chem.Phys.21 714-718

11. Gapon, E.N., 1933 Theory of exchange adsorption V.J.Gen.Chem. (USSR) 3, 667-669, (Chem. Abstr. 28, 4516, 1934)

12. Heier, K., and Ellingsen, K., 1992. Groundwater in Norway, Final Report. The Norwegian Geological Society (NGU). Skrifter 111, 1-36

13. Holtedahl,O.1924: studier over israndterrassene syd for de store Østlandiske sjøer.vid selske.srr.1. Mat.-Naturvidensk. Nr.14

14. Johnson, D.W. and Lindberg, S.E. 1991: Atmospheric deposition and nutrient cycling in forest ecosystems Springer-Verlag New York.

15. Jørgensen, P. and Østmo, S.R., 1990. Hydrogeology in the Romerike area, Southern Norway. Norwegian Geolological Unders. Bulletin 418, 19-26

16. Jørgensen, P., Stuanes, A.O. and Østmo, S.R., 1991 Aqueous geochemistry of the Romerike area, Southern Norway. Norwegian Geolological Unders. Bulletin 420, 57-67.

17. Kim, H.T., 1994. Environmental Soil Science. Marcel Dekker Inc. New York

18. Knudsen, B.S., 2003. Reactive transport of dissolved aromatic compounds under oxygen limiting conditions in sandy aquifer sediments Faculty of Mathematics and Natural Science University of Oslo

19. Longva, O. and Thoresen, M.K.1989: The age of the Hauerseter delta, Norsk geologisk Tidsskrift 69, 131-134

20. Maciej, R.K. 2005. Natural Attenuation of Jet fuel Contaminated Aquifer: Monitoring, field experimentation and Geochemical Modelling. PhD Thesis University of Oslo Faculty of Mathematics and Natural Sciences, University of Oslo Norway

21. McBride, M.B., 1994. Environmental Chemistry of soils, Oxford University Press Oxford New York

22. Otnes, J. 1973. Hydrological data- Norden Romeroke, Norway. Norwegian National Committee for the International Hydrological Decade (IHD). Data volume 1965-1974

23. Otnes, J. 1975: Hydrological data- Norden Romerike, Norway. Norwegian National Committee for the International Hydrological Decade (IHD) Data volume 1972-1974

24. Parkhurst, D.L. and Appelo, C.A.J. 1999. User's guide to PHREEQC (version 2) - a computer program for speciation, batch reaction, one-dimensional transport and inverse geochemical calculations. Water-Resources Investigations Report 99-4259 US Geological Survey

25. Stumm, W., and Morgan, J.J, 1981. Aquatic Chemistry. An introduction Emphasizing Chemical Equilibria in Natural Waters, 3rd edition John Wiley and Sons, INC., New York Chichester Brisbane Toronto Singapore

26. Swensen, B. and Englund J.-O 1996. Unsaturated flow in a heterogeneous deposit, measured by the use of 18O,Cl- and Br- as tracers; paper submitted to the Proceedings to the Jens Olaf Englund Seminar "Protection of groundwater resources against contaminants" Edited by Per Aagaard and K.J. Tuttle Gardermoen Norway

27. Sørensen, R. 1979: late Weichselian deglaciation in the Oslofjord area, Southern Norway. Boreas 8, 241-246

28. Søvik, A.K., 2001. Transport and Degradation in Unsaturated Heterogeneous Media- Variability of Microbial Degradation of Organic Contaminants. Faculty of Mathematics and Natural Science University of Oslo

29. Tuttle, K.J., 1997. Sedimentological and hydrogeological characterization of a raised ice contact delta- the Preboreal delta-complex at Gardermoen, Southern Norway. Doc.Scie. University of Oslo Norway

30. Vanselow, A.P., 1932. Equilibra of the base exchange reactions of bentonites, permutites, soil colloids and zeolites, Soil Science 33, 95-113. 1932.

31. Williams, J.D., 1997. Groundwater Geochemistry: Fundamentals and Applications to Contamination CRC Press LLC Florida US

32. Yong, R.N Geoenvironmental Engineering: Contaminated soil. Pollutant fate and mitigation, CRC Press 2000 Retrieved 23/01/06 from www.environetbase.com//books/77/8289_PDF_CO2.pdf

33. Yong, S.C, Ahmed H., David H.F.L, Kent K.M , Environmental Engineers handbook, 2nd Edition Retrieved 23/01/2006 from http://www.environetbase.com//books/78/ch09.pdf

34. Østmo. S.R 1977: rapport vedrørende kvartærgeologosk kartleggind med spesiell vekt på registering og underso\økelse av sand-og grusforekomster I Ullensaker Kommune, Akershus fluke, norges geologiske Undersøkelse, rapport 0-75 045

List of Annexes

Annex I Borehole log for the well where the soil samples are taken

LOG OF BORING

GAEA Technologies Ltd.
202, 1614 Dundas Street E.
Whitby, Ontario, Canada L1N 8Y8

PROJECT: **Tålegrenseprosjektet**

BORING: Ved BR_S

LOCATION
Øst for østre bane

DATE: 16/11-05

SCALE: m

ELEV.	Depth	Description of Materials	BPF	WL	Remarks
0.0	0	Ground Surface			
		Grus og sand Ikke prøvetatt			
-3.0					Prøve nr 6
-4.0		Grus 45,5% Sand 31,4%			
	5	Grusig sand Ikke prøvetatt			
-6.0					Prøve nr 7
-7.0		Sand 50,6% Grus 40,8%			
-8.0		Grusig sand Ikke prøvetatt			
-9.0		Fin-/mellomsand Ikke prøvetatt			
-10.0		Mellomsand 51,3% Finsand 38,1%			Prøve nr 8
	10	Fin-/mellomsand Ikke prøvetatt			
-12.0					Prøve nr 9
-13.0		Finsand 43,0% Mellomsand 42,3% Silt 10,6%			
		Fin-/mellomsand Ikke prøvetatt			Grunnvannsspeil ved 13,8 m
-15.0	15				Prøve nr 10
-16.0		Mellomsand 57,5% Finsand 27,3% Grovsand 10,1%			
		Fin-/mellomsand Ikke prøvetatt			
-18.0					Prøve nr 11
-19.0		Mellomsand 51,3% Finsand 38,1%			
		Fin-/mellomsand Ikke prøvetatt			
-21.0	20				Prøve nr 12
-22.0		Finsand 59,5% Mellomsand 24,8% Silt 14,5%			

Annex II Procedure of CEC determination and results obtained from the laboratory analysis

Result of Ion Exchange Analyses of Soil Samples from Gardermoen
Procedures**

1. **Dry the soil samples in an oven at 30^{o}C**
2. **Sieve the soil samples in 2mm sieve and weigh 25g of the sample**
3. **Add 1M NH_4NO_3 solution into the soil and put the mixture in a shaking for the whole night**
4. **Filter the mixture after a night of shaking and add 1M NH_4NO_3 until a 250ml extract is prepared**
5. **Analyse the extract with respect to various cations using Atomic Absorption Spectrometery**

Laboratory Result for the soil samples												
Samples	Depth(m)	TC	TOC	TIC	Ca++	Mg++	Na+	K+	Fe++	Al+++	H+	CEC (meq/100g soil)
6	3.5	0	0	0	1.05	0.303	0.039	0.105	0.005	0.016	0.00235	1.52
7	6.5	0.38	0.14	0.24	2.5	0.308	0.031	0.074	0.006	0.012		2.93
8	9.5	0.24	0.10	0.13	2.06	0.197	0.017	0.059	0.002	0.011	0.00136	2.35
9	12.5	0.14	0.09	0.05	1.17	0.322	0.015	0.061	0.000	0.009	0.00117	1.58
10	15.5	0.35	0.12	0.23	3.15	0.172	0.047	0.051	0.005	0.018		3.44
11	18.5	0.30	0.14	0.16	2.75	0.139	0.019	0.046	0.001	0.009		2.96
12	21.5	0.55	0.25	0.30	2.85	0.219	0.017	0.064	0.000	0.008		3.16

** Ogner et.al 2000 The chemical Analysis Program of the norwegian Forest Research Institute pp 13

Annex III Snow composition used as influent solution

Sample ID	Location	Sampling Date	Formate		PG	
			mg/l	mol/l	mg/l	mol/l
M006-00130-008	15 m v/B6	230106	522	7.68	2560	33.64
M006-00256-008	15 m v/B6	30206	414	6.09	3080	40.47
M006-00342-008	15 m v/B6	130206	234	3.44	1080	14.19
M006-00436-008	15 m v/B6	240206	374	5.50	1180	15.51
M006-00674-008	15m v/B6	270306	46.2	0.68	179	2.35
M006-00130-007	30 m v/B6	230106	248	3.65	2180	28.65
M006-00256-007	30 m v/B6	30206	303	4.46	2020	26.54
M006-00342-007	30 m v/B6	130206	433	6.37	941	12.37
M006-00436-007	30 m v/B6	240206	176	2.59	827	10.87
M006-00674-007	30m v/B6	270306	22.9	0.34	255	3.35
		Total Sum	2773.1	40.78	14302	187.94
		Average	277.31	4.078	1430.2	18.794

Annex IV Composition of Groundwater from Br_S used as a pore solution

Well	Element	Concentration	
		mg/l	mmol/l
Br_S	Cl-	5.05	0.142
Br_S	Ca++	215	5.375
Br_S	Alkalinity		6.21*
Br_S	A+++	0.04646	0.002
Br_S	Na+	6.39	0.278
Br_S	Mn	0.008	0.000
Br_S	Mg++	9.81	0.404
Br_S	K+	1.66	0.042
Br_S	Fe++	0.222	0.004
Br_S	SO4--	10.6	0.110
Br_S	NO3-	18	0.290
Br_S	NH4+	0.01	0.001
Br_S	OXYGEN	9.79	0.306
Br_S	TEMP	6.7	Celsius
Br_S	PH	7.19	pH

Annex V Major Minerals identified by XRD analysis of the soil samples

Sample No 6

Visible	Ref. Code	Score	Compound Name	Displacement [°2Th.]	Scale Factor
*	46-1045	63	Quartz, syn	0,000	0,989
*	09-0466	51	Albite, ordered	0,000	0,161
*	07-0042	46	Muscovite-	0,000	0,043
*	38-0359	26	Magnesiosadan agaite	0,000	0,012
*	07-0076	52	Clinoclore, ferroan	0,000	0,026
*	10-0357	39	Sanidine, K-	0,000	0,066

Sample No 7

Visible	Ref. Code	Score	Compound Name	Displacement [°2Th.]	Scale Factor
*	46-1045	65	Quartz, syn	0,000	0,985
*	20-0554	53	Albite	0,000	0,105
*	29-0701	42	Clinochlore-	0,000	0,021
*	07-0042	40	Muscovite-	0,000	0,032
*	01-0705	40	Microcline	0,000	0,103
*	38-0359	30	Magnesiosadan agaite	0,000	0,010
*	43-0685	26	Illite-	0,000	0,080
*	08-0048	38	Orthoclase	0,000	0,027

Sample No 8

Visible	Ref. Code	Score	Compound Name	Displacement [°2Th.]	Scale Factor
*	46-1045	60	Quartz, syn	0,000	0,808
*	20-0554	50	Albite, ordered	0,000	0,068
*	01-0705	39	Microcline	0,000	0,075
*	09-0343	29	Illite,	0,000	0,057
*	07-0032	33	Muscovite	0,000	0,060
*	02-0108	23	Chamosite	0,000	0,015
*	50-1686	18	Fluororichterite	0,000	0,155

Sample No 9

Visible	Ref. Code	Score	Compound Name	Displacement [°2Th.]	Scale Factor
*	46-1045	56	Quartz, syn	0,000	0,988
*	20-0554	51	Albite, ordered	0,000	0,085
*	01-1098	42	Muscovite	0,000	0,041
*	01-0705	33	Microcline	0,000	0,099
*	07-0076	25	Clinoclore, ferroan	0,000	0,011
*	29-1258	13	Ferrohornblend	0,000	0,010

Sample No 10

Visible	Ref. Code	Score	Compound Name	Displacement [°2Th.]	Scale Factor
*	46-1045	65	Quartz, syn	0,000	0,985
*	41-1480	50	Albite, Ca-rich,	0,000	0,085
*	05-0586	38	Calcite, syn	0,000	0,020
*	12-0088	23	Ankerite	0,000	0,004
*	29-0701	31	Clinochlore	0,000	0,011
*	07-0042	43	Muscovite	0,000	0,026
*	01-0705	34	Microcline	0,000	0,105
*	41-0586	29	Ankerite	0,000	0,006

Sample No 11

Visible	Ref. Code	Score	Compound Name	Displacement [°2Th.]	Scale Factor
*	46-1045	66	Quartz, syn	0,000	0,981
*	20-0554	50	Albite, ordered	0,000	0,056
*	09-0343	37	Illite,	0,000	0,010
*	09-0478	38	Anorthoclase,	0,000	0,044
*	07-0076	38	Clinoclore, ferroan	0,000	0,009

Sample No 12

Visible	Ref. Code	Score	Compound Name	Displacement [°2Th.]	Scale Factor
*	46-1045	56	Quartz, syn	0,000	0,898
*	09-0466	45	Albite, ordered	0,000	0,092
*	01-0705	35	Microcline	0,000	0,086
*	09-0343	25	Illite,	0,000	0,051
*	07-0076	25	Clinoclore, ferroan	0,000	0,011
*	50-1686	19	Fluororichterite	0,000	0,185

Annex VI PHREEQC input file for infiltration of Na-formate solution in the unsaturated zone at Gardermoen

```
TITLE Gardermoen ion exchange and transport
SOLUTION_MASTER_SPECIES
Formate HFormate 0.0 Formate- 45
SOLUTION_SPECIES
HFormate =  HFormate
      -gamma      3.5   0.015
      log_k 0
      -delta_H    0     kJ/mol      # Calculated enthalpy of
reaction   HAcetate
Formate- =  Formate-
      -gamma      3.5   0.015
      log_k 0
      -delta_H    0     kJ/mol      # Calculated enthalpy of
reaction   HAcetate
HFormate =  Formate- + H+
         log_k         -3.75
      -delta_H    0                 # Not possible to calculate
enthalpy of reaction  Acetate-
#     Enthalpy of formation:      -0 kcal/mol
SOLUTION 0  Water with Na formate
        units             mmol/kgw
        temp            25
        pH              7.0     charge
        pe              12.5    O2(g)   -0.68
        Na              7.68
         Formate        7.68

SOLUTION 1-22  Initial solution for column
         units              mmol/kgw
        temp               25.0
        pH                 7.19
        pe                 12.5    O2(g)   -0.68
        Ca                 5.375
        Cl                 0.142
         S(6)               0.11
        N(5)               0.29
        Alkalinity         6.21
        Na                 0.278
        K                  0.042
        Mg                 0.404
        Fe                 0.004
EXCHANGE 1-4
    CaX2 0.69
    MgX2 0.2
    NaX  0.03
    KX   0.07
#         -equilibrate 1-4
EXCHANGE 5-7
    CaX2 0.85
    MgX2 0.11
    NaX  0.01
```

```
   KX   0.03
#        -equilibrate 5-7
 EXCHANGE 8-10
   CaX2 0.88
    MgX2 0.08
    NaX  0.01
  KX   0.03
#         -equilibrate 8-10
EXCHANGE 11-13
    CaX2 0.74
    MgX2 0.20
    NaX  0.01
 KX   0.04
#        -equilibrate 11-13
EXCHANGE 14-16
    CaX2 0.91
    MgX2 0.05
    NaX  0.01
  KX   0.01
#      -equilibrate 14-16
EXCHANGE 17-19
    CaX2 0.93
    MgX2 0.05
    NaX  0.01
  KX   0.02
#      -equilibrate 17-19
EXCHANGE 20-22
    CaX2 0.90
    MgX2 0.07
    NaX  0.01
   KX   0.02
#     -equilibrate 20-22
RATES
S_degradation
#dS/dt = -k_max*S/(k_half + S), K_max is maximum growth rate,
mol formate/L/s
# S is formate conc; mol/L       k_half is half saturation
conc, mol formate/L
-start
1 k_max = parm(1); 2 k_half = parm(2); # parms defined in
KINETICS
10 S = tot ("Formate")
20 if S < 1e-9 then goto 50
30 rate = -k_max*S/(k_half + S)
40 dS = rate * time
50 save dS
-end
END
KINETICS 1-22
      S_degradation
      -formula Formate 1 C -1 O -2 H -1
       -m  0.0076
      -parms     1.7e-9     1.8e-5
      -tol 1e-5
     -step_divide 5
     -runge_kutta 2
```

```
PRINT
-reset false
SELECTED_OUTPUT
      -file IonExch.sel
      -totals Ca Mg Na K Cl
TRANSPORT
-cells 22
-lengths 1
-shifts 14
-time_step 172800
-flow_direction forward
-boundary_conditions flux flux
-dispersivities 0.02
-diffusion_coefficient 1e-9
-print_cells 1-22
-print_frequency 14
-punch_cells 1-22
-punch_frequency 14
USER_GRAPH
      -headings Distance Ca Mg Na K Formate Cl
     -chart_title "Cation Exchange & Formate biodegradation"
      -axis_scale x_axis 0 22 2
      -axis_scale y_axis 0 8 0.5
      -axis_titles "Depth (m)" "Concentration (mmol/l)"
      -initial_solutions false     # no plot of initial
equilibrations
-start
# The PHREEQC-2 BASIC statements
  10 graph_x Dist
  20 graph_y TOT("Ca")*1000, TOT("Mg")*1000, TOT("Na")*1000,
TOT("K")*1000, TOT("Formate")*1000,TOT("Cl")*100 #,
MOL("Mn+2")*1000, MOL("Fe+2")*1000,TOT("Ca")*1000,
TOT("Na")*1000, TOT("Cl")*1000, TOT("K")*1000,TOT("Mg")*1000
  -end
END
```

Annex VII Batch experiment on biodegradation of formate

```
TITLE Gardermoen Formate biodegradation
SOLUTION_MASTER_SPECIES
Formate HFormate 0.0 Formate- 45
SOLUTION_SPECIES
HFormate =  HFormate
      -gamma      3.5   0.015
      log_k 0
      -delta_H    0     kJ/mol      # Calculated enthalpy of
reaction   HAcetate
Formate- =  Formate-
      -gamma      3.5   0.015
      log_k 0
      -delta_H    0     kJ/mol      # Calculated enthalpy of
reaction   HAcetate
HFormate =  Formate- + H+
         log_k         -3.75
      -delta_H    0                 # Not possible to calculate
enthalpy of reaction  Acetate-
#     Enthalpy of formation:      -0 kcal/mol
RATES
S_degradation
#dS/dt = -k_max*S/(k_half + S), K_max is maximum growth rate,
mol formate/L/s
# S is formate conc; mol/L        k_half is half saturation
conc, mol formate/L
-start
1 k_max = parm(1); 2 k_half = parm(2); # parms defined in
KINETICS
10 S = tot ("Formate")
20 if S < 1e-9 then goto 50
30 rate = -k_max*S/(k_half + S)
40 dS = rate * time
50 save dS
-end
SOLUTION 1  Water with Na formate
        units             mmol/kgw
        temp          10
        pH              7.19
        pe              12.5    O2(g)   -0.68
        Na               7.68
         Formate      7.68
       Ca               5.375
        Cl               0.142 charge
          S(6)            0.11
        N(5)            0.29
        Alkalinity      7.8
        K                 0.042
        Mg              0.404
EXCHANGE 1
    CaX2 0.85
    MgX2 0.11
    NaX  0.01
   KX   0.03
```

```
KINETICS 1
      S_degradation
      -formula Formate 1 C -1 O -2 H -1
       -m  0.0076
      -parms     1.7e-9     1.8e-5
     -steps 5e6 in 40
INCREMENTAL_REACTIONS true
USER_GRAPH
 -chart_title "Formate biodegradation in a batch system"
 -headings time Formate #Ca Mg Na K
 -axis_titles "Time / days" "mmol Formate/ L"
-axis_scale x_axis 0 60 10
-axis_scale y_axis 0 10 1

 -start
 10 graph_x total_time / 86400
 20 graph_y tot("Formate") * 1e3#, TOT("Ca")*1000,
TOT("Mg")*1000, TOT("Na")*1000, TOT("K")*1000
 -end
END
```